Specific heat of ^{4}He and ^{3}He-^{4}He mixtures at their λ transition*

F. M. Gasparini†
Department of Physics and Astronomy, State University of New York at Buffalo, Buffalo, New York 14214

M. R. Moldover‡
School of Physics and Astronomy, University of Minnesota, Minneapolis, Minnesota 55455

(Received 2 December 1974)

We have measured the specific heat near the λ transition of pure ^{4}He and of five ^{3}He-^{4}He mixtures up to a mole fraction of 0.39 ^{3}He in ^{4}He. Our data for ^{4}He confirm the results of Ahlers revealing an asymmetry in the exponents above and below T_λ when the specific heat is represented by a simple-power-law temperature dependence. Our results for these exponents ($\alpha = 0.012 \pm 0.002$ and $\alpha' = -0.012 \pm 0.004$) differ somewhat from Ahlers's. Our results can be reconciled with the requirement of scaling ($\alpha = \alpha'$) only by supposing substantial contributions to C_p are made by singular correction terms to a simple power law. The measured specific heat of the mixtures richest in ^{3}He appears to be finite, continuous, and cusped at the λ line. These qualitative features have been termed "renormalization" by Fisher. An analysis of our mixture data with a power-law temperature dependence does not yield a fully renormalized exponent, but rather an effective exponent. We have calculated the following derivatives at the λ line: $(\partial s/\partial T)|_{p,\lambda}$, $(\partial\phi/\partial T)|_{p,\lambda}$, and $(\partial x/\partial T)|_{p,\lambda}$. We have used these derivatives to calculate the specific heat along paths of constant pressure and constant relative chemical potential $C_{p\phi}$. This specific heat behaves very much like C_p of pure ^{4}He supporting the idea of universality for the specific-heat exponents. It is also true that the same asymmetry in the branches above and below T_λ which is observed in pure ^{4}He is retained in the mixtures. The persistence of the asymmetry of $C_{p\phi}$ as one moves along the λ line towards increasing ^{3}He concentration (at the saturated vapor pressure of the mixtures) is analogous to the persistence of the asymmetry of C_p as one moves along the λ line towards increasing pressure in pure ^{4}He. In both cases a unique reconciliation of the asymmetry with scaling must await better predictions of the form of the corrections to scaling. We have used our calculated $C_{p\phi}$ to construct the derivative $(\partial x/\partial T)|_{p,\phi}$ hence paths of constant ϕ on the x-T plane, as well as the derivative $(\partial x/\partial\phi)|_{p,T}$.

I. INTRODUCTION

The superfluid or λ transition of pure liquid ^{4}He is characterized by the well-known nearly logarithmic behavior of the specific heat at constant pressure C_p. The classic measurements of Fairband, Buckingham, and Kellers[1] showed that as close as 10^{-6} K to the λ transition the specific heat continues to rise and appears to diverge as $\ln|T - T_\lambda|$. In contrast to the situation for pure ^{4}He, early specific-heat measurements at the superfluid transition of the ^{3}He-^{4}He mixtures showed no divergence of C_p at the λ line. These measurments had been interpreted to mean that the λ transition in helium mixtures is a classical second-order transition with the specific heat having a discontinuity.[2] A review of the data available up to 1964 is given by Taconis and de Bruyn Ouboter.[3] More recently, measurements of the composition of helium mixtures in the liquid and vapor phases in equilibrium have been made as close as 1 mK to T_λ.[4] Once again the experimenters concluded that the λ transition is a classical second-order Ehrenfest transition with discontinuities in C_{px}, dp/dT, etc. (Here C_{px} is the specific heat of constant pressure and constant mole fraction of ^{3}He, x.) Contrary to these conclusions, our specific-heat measurements show that at fixed ^{3}He concentration, C_{px} is continuous across the λ transition. We also find that C_{px} is singular, reaching a finite value with infinite slope at the λ transition (see Fig. 1). A preliminary account of this work stating these qualitative conclusions has been published.[5] To the preliminary account we now add a detailed description of our experiments and the analysis of our data to accurately extract C_{px}. We also examine the behavior of C_{px} in light of "scaling" and "universal" descriptions of phase transitions. In order to do this we have calculated $C_{p\phi}$, the specific heat at constant pressure and constant chemical potential difference, $\phi \equiv \mu_3 - \mu_4$. Our measurements extend to a mole fraction of $x = 0.39$ and do not explore the region of the tricritical point where the line of superfluid transitions meets the phase separation lines. Specific-heat data near the tricritical point have been reported in Ref. 6.

The effect of ^{3}He on the superfluid transition of ^{4}He can be viewed as an example of renormalization of a phase transition, a concept first introduced by Fisher.[7] According to this the ^{3}He is viewed as a mobile impurity whose concentration fluctuates in equilibrium with the ^{4}He system undergoing a phase transition. The impurity gives the system a new degree of freedom but does not

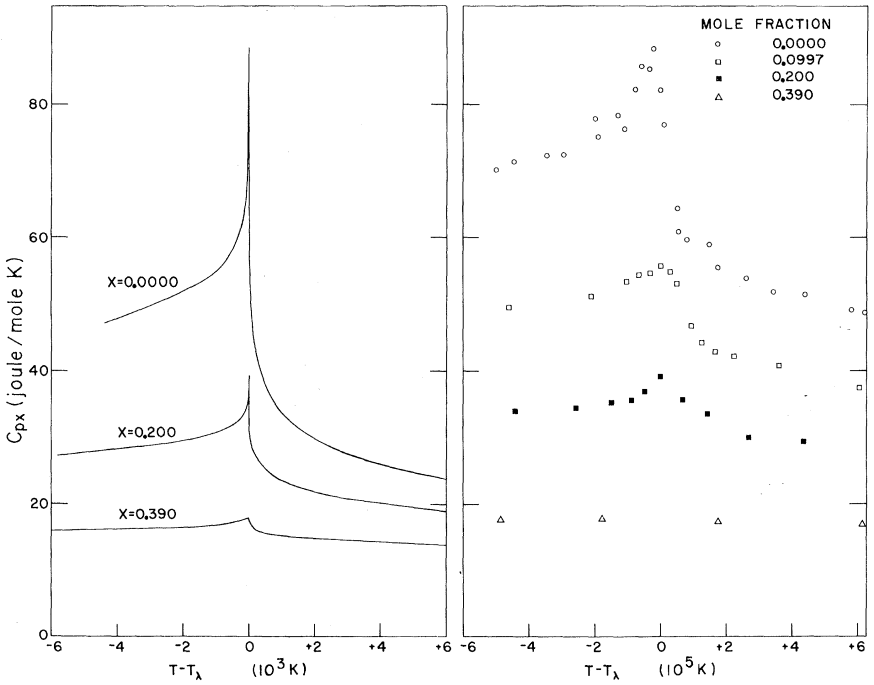

FIG. 1. Specific heat (at constant pressure and composition) of some mixtures of ^{3}He in ^{4}He and the constant-pressure specific heat of ^{4}He. The data are shown on two different linear temperature scales.

participate in an essential way in the critical nature of the phase transition. The presence of ^{3}He depresses the λ temperature and affects the coefficients of the specific-heat singularity, but is expected to leave its asymptotic temperature dependence unaltered; i.e., the specific heat is expected to behave just like that of pure ^{4}He. This behavior is realized under the important proviso that the measurements be made along a particular thermodynamic path, which in this case is that of constant ϕ, the difference in the molar chemical potential of the two components. Along the thermodynamically conjugate path of constant mole fraction, x, the specific heat is "renormalized." Thus if $C_{p\phi}$ diverges as $|T-T_\lambda(p,\phi)|^{-\alpha} \equiv \theta^{-\alpha}$ where $\alpha>0$, then C_{px} is finite, behaving as $|T-T_\lambda(p,x)|^{\alpha/(1-\alpha)} \equiv t^{\alpha/(1-\alpha)}$. (By the symbol θ we mean the temperature difference between two equilibrium states of the helium mixture, one state at temperature T, pressure p, and chemical potential difference ϕ, and a second state with the same values of p and ϕ but at the λ temperature. Similarly, t is a temperature difference taken at constant p and x.) Our data support the applicability of the ideas of renormalization to the λ transition in helium mixtures, particularly the assumed behavior of $C_{p\phi}$. Our data cannot be used to extract the asymptotic renormalized behavior. This difficult, if not impossible, task arises from the very weakness of the singularity in C_p and has been discussed in Ref. 8. Although the term "renormalization" was introduced in a statistical-mechanics context, we shall see that similar conclusions may be reached from certain thermodynamic arguments. Indeed, Lipa and Buckingham[9] predicted the qualitative behavior of C_{px} which we observe (Fig. 1) from just such arguments. Our results can also be considered an illustration of the general considerations applying to critical points in multicomponent systems, which have been discussed by Griffiths and Wheeler.[10]

Prior to our measurements on the mixtures we made control experiments on pure ^{4}He, expecting to obtain the results of Ref. 1. We actually found ourselves in slight disagreement with the earlier conclusion of a symmetric logarithmic divergence. Ahlers has already reported[11] similar results from his own measurements on ^{4}He and has discussed their implications for scaling laws. Our own measurements are of a precision comparable to those of Ahlers and tend to confirm his conclusions, although differing somewhat in details. We find, upon fitting to a simple power law data from the branches of the specific heat C_p above and below the superfluid transition temperature, the unequal exponents $\alpha = 0.012 \pm 0.002$ and $\alpha' = -0.012 \pm 0.004$, respectively. This exponent inequality or asymmetry persists in the specific-heat $C_{p\phi}$ as one moves along the λ line towards increasing ^{3}He mole fraction. Such an asymmetry is in conflict with the *simplest* interpretation of scaling, which predicts $\alpha = \alpha'$; however, the persistence of the asymmetry does support the hypothesis of "universality," i.e., that the functional form of the specific heat does not change as an inert variable (such as ^{3}He concentration) is changed. To reconcile the $C_{p\phi}$ calculated from our data with scaling, one must sup-

pose that there exist singular correction terms to the power-law behavior of the specific heat at the λ line. These terms must contribute significantly to $C_{p\phi}$ even in the temperature region closest to T_λ.

The rest of this paper is organized as follows. In Sec. II we discuss some of the relevant thermodynamics of the λ transition for mixtures. Here we also present the results of our computing derivatives along the λ line which were found necessary for later analysis. In Sec. III we present details of our apparatus and the experimental procedure. The data are then discussed and analyzed in Sec. IV. Here we calculate the specific heat C_p for pure ^{4}He and the specific heat C_{px} for ^{3}He-^{4}He mixtures. In Sec. V we calculate $C_{p\phi}$ and discuss it in terms of scaling and universality. In Sec. VI we compute the derivatives $(\partial x/\partial T)|_{p,\phi}$ and $(\partial x/\partial\phi)|_{p,T}$. The paper ends with Sec. VIII, in which we summarize our results.

II. THERMODYNAMICS AND RENORMALIZATION

In the presence of ^{3}He the locus of superfluid transitions, which for the pure system had been a line in p-T space, becomes a surface. This surface in p, T, x space can, however, be reduced to a line if one considers the pressure to be fixed or, as is usually done, the pressure to be the saturated vapor pressure of the mixture. The complication of the extra dimension can thus be avoided and all of the thermodynamics developed for λ lines[12] can be used for the mixtures. Formally one can start from the differential of the molar Gibbs free energy,

$$dg = -s\,dT + v\,dp + \mu_3\,dx + \mu_4\,d(1-x)\,, \tag{1}$$

where s and v are the molar entropy and volume and μ_3 and μ_4 are the molar chemical potentials. Introducing the relative chemical potential ϕ one has

$$dg = -s\,dT + v\,dp + \phi\,dx\,, \tag{2}$$

with ϕ being the variable conjugated to the concentration. At constant pressure, Eq. (2) becomes analogous to the differential of the Helmholtz free energy of a one-component system with the identification ϕ to $-p$ and x to v. One can then readily write down a relationship between C_{px} and $C_{p\phi}$ which is implicit in the work of Ref. 12:

$$C_{p\phi} = C_{px}\,\frac{\left(T\frac{\partial x}{\partial T}\Big|_{p,t}\frac{\partial\phi}{\partial T}\Big|_{p,t} - T\frac{\partial s}{\partial T}\Big|_{p,t}\right)+\left(T\frac{\partial s}{\partial T}\Big|_{p,t}\right)^2}{T\frac{\partial s}{\partial T}\Big|_{p,t} + T\frac{\partial x}{\partial T}\Big|_{p,t}\frac{\partial\phi}{\partial T}\Big|_{p,t} - C_{px}}\,. \tag{3}$$

The partial derivatives at constant t are along a path which at constant pressure is parallel to the λ line in x-T space. Equation (3) is a very convenient way of relating an easily measured specific heat C_{px} to another, $C_{p\phi}$, which is less accessible via derivatives which have a weak temperature dependence near the transition. Indeed, it is a good approximation in a small enough temperature neighborhood near T_λ to use the value of these derivatives at $t=0$. We indicate these derivatives at $t=0$ by the subscript λ, i.e., $(\partial s/\partial T)|_{p,\lambda}$. The pressure is explicitly indicated as being constant in Eq. (3). In practice, however, when calculating the derivatives along the λ line ("λ derivatives") one makes use of data obtained with liquid and vapor coexisting. If these data are taken (as is frequently the case) as a function of temperature in a constant-volume system nearly filled with liquid but with the vapor phase present, the data are along a unique path in T-p-x_{liquid} space. This path is nearly a path of constant x_{liquid} at saturated vapor pressure, but not quite, because the vapor and liquid concentrations differ, leading to a change in liquid composition as the vapor pressure changes with temperature. In our region of interest these differences are unimportant. For instance in the range of our measurements at any given concentration the vapor pressure varied by about 1 mbar, while the vapor pressure itself was about 50 mbar. This small a variation has a negligible effect on any of the thermodynamic derivatives. In Table I we have listed estimates of these λ derivatives. To obtain $(\partial x/\partial T)|_{p,\lambda}$ we have differentiated the data on the λ transition as a function of concentration compiled by Sydoriak and Roberts.[13] For $(\partial s/\partial T)|_{p,\lambda}$ we have integrated the available heat-capacity data[2,14] up to T_λ at several mole fractions. The resulting entropy–mole-fraction curve was then graphically smoothed and differentiated. For $(\partial\phi/\partial T)|_{p,\lambda}$ we have used the expression[15]

$$\phi(p,T,x) = \mu_0^3(p_0^3,T) - \mu_0^4(p_0^4,T) + RT\ln[x/(1-x)] + \phi^E(T,p,x)\,, \tag{4}$$

where μ_0^3 and μ_0^4 are, respectively, the chemical potentials of pure ^{3}He and ^{4}He evaluated at their respective pressures corresponding to the temperature T. The excess chemical potentials were obtained from the work of Roberts and Swartz.[16] To obtain $(\partial\phi/\partial T)|_{p,\lambda}$ from Eq. (4) we used the identity

$$\frac{\partial\phi}{\partial T}\Big|_{p,\lambda} = \left(\frac{\partial\phi}{\partial x}\Big|_{p,T} + \frac{\partial\phi}{\partial T}\Big|_{p,x}\frac{\partial T}{\partial x}\Big|_{p,\lambda}\right)\frac{\partial x}{\partial T}\Big|_{p,\lambda}\,. \tag{5}$$

The relationship between $C_{p\phi}$ and C_{px} of Eq. (3) is also useful to examine the renormalization ideas discussed in the Introduction. Except at $x=0$ where $(\partial\phi/\partial T)|_{p,\lambda}$ diverges as $1/x$, all the λ derivatives are finite along the λ line. Furthermore, we note that the coefficient of C_{px} in the numerator of Eq. (3) is always positive; hence the quantity

$$C_{\max} = T_\lambda\frac{\partial s}{\partial T}\Big|_{p,\lambda} + T_\lambda\frac{\partial x}{\partial T}\Big|_{p,\lambda}\frac{\partial\phi}{\partial T}\Big|_{p,\lambda} \tag{6}$$

TABLE I. Our estimate of the λ-line parameters at various mole fractions. These are the parameters used in the data analysis.

x	T_λ (K)	$\left.\frac{\partial x}{\partial T}\right\|_{p,\lambda}$ (K^{-1})	$\left.\frac{\partial \phi}{\partial T}\right\|_{p,\lambda}$ (J $mole^{-1}$ K^{-1})	$\left.\frac{\partial s}{\partial T}\right\|_{p,\lambda}$ (J $mole^{-1}$ K^{-2})
0.0110	2.157	-0.714 ± 0.007	-1200 ± 21	-20.9 ± 4.2
0.0997	2.027	-0.667 ± 0.006	-140.7 ± 2.6	-13.9 ± 2.6
0.200	1.872	-0.621 ± 0.006	-69.7 ± 1.6	-7.6 ± 2.3
0.301	1.700	-0.559 ± 0.006	-42.5 ± 1.2	-3.0 ± 2.2
0.39	1.532	-0.500 ± 0.005	-30.1 ± 0.7	$+0.15\pm1.5$
0.53	1.223	-0.424 ± 0.004	-16.6 ± 0.5	$+2.34\pm0.5$

must form the upper bound for C_{px}. Were C_{px} to exceed this, we would have a negative $C_{p\phi}$, in violation of thermodynamic stability. That C_{px} cannot diverge all along a line of second-order phase transitions has been shown rigorously by Wheeler and Griffiths.[17] From thermodynamics there are no such restrictions on $C_{p\phi}$. It is clear, however, that if C_{px} reaches its upper bound then $C_{p\phi}$ will be infinite. The way it diverges is a matter of conjecture. If one assumes $C_{p\phi}\sim\theta^{-\alpha}$, $\alpha>0$, then one can readily show that Fisher's renormalization result, $C_{px}\sim t^{\alpha/(1-\alpha)}$, follows from Eq. (3) and the fact that one must also have $(\partial x/\partial T)|_{p,\phi}\sim\theta^{-\alpha}$. The latter is obtained from the identity

$$\left.\frac{\partial x}{\partial T}\right|_{p\phi} = -\frac{1}{T}\left.\frac{\partial T}{\partial \phi}\right|_{p,t} C_{p\phi} + \left.\frac{\partial s}{\partial T}\right|_{p,t}\left.\frac{\partial T}{\partial \phi}\right|_{p,t}. \qquad (7)$$

To show how C_{px} is renormalized one expands Eq. (3) in terms of $1/C_{p\phi}$ which immediately yields the leading term $C_{px}^{\phi}\sim\theta^{\alpha}$, where we have indicated by the superscript that this is C_{px} along the path ϕ = const. The path correction to bring C_{px}^{ϕ} into C_{px} can be done using Eq. (7) and results in $C_{px}\sim t^{\alpha/(1-\alpha)}$. This procedure is outlined in Ref. 7 and we will come back to it in Sec. V, where we concern ourselves with the reverse process of taking C_{px} into $C_{p\phi}$. It becomes clearer now why the renormalization exponent $\alpha/(1-\alpha)$ is so hard to measure. The exponent appears in the leading term of a series whose convergence is determined by the strength of the divergence of $C_{p\phi}$. The divergence of $C_{p\phi}$ is nearly logarithmic. This is so weak that the fully renormalized C_{px} occurs in a region so close to T_λ that it is experimentally inaccessible. Thus for a full test of renormalization, it would be much better to measure the assumed most divergent thermodynamic derivatives [$(\partial x/\partial T)|_{p,\phi}$, etc.] and to test directly the conjecture that no matter where one crosses the λ line these derivatives show the same nearly logarithmic divergence as does C_p in pure ^{4}He. Our own approach to the question of renormalization is to use C_{px} to construct $C_{p\phi}$, as we will do in Sec. V.

III. APPARATUS AND EXPERIMENTAL PROCEDURE

A. Calorimeter

A good calorimeter should have small heat capacity relative to the sample being measured; it should be built of high-conductivity material to ensure isothermal conditions; it should be well isolated from its surrounding; and in our specific case it should be so constructed as to allow quick changes of sample. The calorimeter shown in Fig. 2 satisfies all these requirements and incorporates an arrangement briefly described in Ref. 5 in which a needle valve is made part of the calorimeter. This feature allows one to seal the calorimeter chamber and evacuate the connecting capillary. Troublesome effects due to the superfluid film flow or to part of the sample being in the filling capillary are thus eliminated.[18]

The calorimeter consists of two pieces of oxygen-free high-conductivity (OFHC) copper held together by eight screws. The vacuum seal is made with a 0.075-cm indium O ring. When the sample is condensed through the filling capillary, it resides in slots cut into the calorimeter bottom.[19] In this arrangement the condensed sample is at no point farther than 0.035 cm from a copper surface. Two bottoms were used in the course of the experiment. The calorimeter with the slotted bottom piece, calorimeter (1), had a volume of 1.998 ± 0.002 cm^3 and was used for measurements on ^{4}He and on the mixtures with mole fractions 0.0110, 0.0997, 0.2000, and 0.390. Calorimeter (2) used an unslotted bottom piece and had a volume of 1.305 ± 0.001 cm^3. It was used for measurements on ^{4}He and on the mixtures with mole fraction 0.30. The heights over which the liquid extended in these calorimeters were 0.35 and 0.1 cm, respectively. The performance of the two calorimeters was identical except for a slight difference in the relaxation times. Calorimeter (1) had a relaxation time both above and below T_λ less than the time constant in the thermometer circuit, 0.3–3 sec. Calorimeter (2) performed in the same way

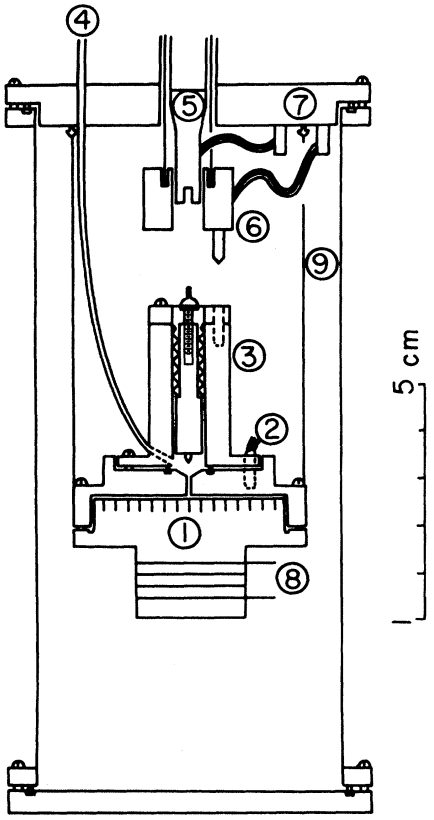

FIG. 2. Schematic representation of the calorimeter in the vacuum can. The screwdriver (5) and countertorque (6) are used to cool down the calorimeter as well as to operate the needle value assembly (3). Other parts indicated are calorimeter bottom(1), resistance thermometer (2), filling capillary (4), flange of vacuum can (7), heater (8), and nylon support thread (9).

for the measurements on ^{4}He but had a noticeable time constant of about 3–5 sec for the measurements on the mixture. This time constant was of no consequence.

The needle value assembly is located on top of the calorimeter and sealed to it with an indium *O* ring. The needle of this valve was machined to size from a standard valve stem. The stem is soldered into a carefully machined "guide," which allows the needle to move up and down without turning or becoming misaligned. The guide is soldered to a small commerically manufactured[20] bellows which serves as a stem seal (or packing) and prevents rotation. The guide is translated with a modified screw arrangement. The screw is captive on top of the calorimeter assembly, and engages a threaded hole in the top of the guide. To translate the guide a slotted screwdriver is lowered and turned. The calorimeter is suspended on nylon strings, for good thermal isolation. Thus the operation of the needle valve necessitates the use of a countertorque. This countertorque engages in three holes on top of the valve assembly and holds the calorimeter while the screw is being turned. Since no exchange gas is used inside the vacuum can, the calorimeter is cooled by making mechanical contact with the countertorque. The countertorque itself is thermally connected with fine copper wires to a post extending from the flange in contact with the surrounding ^{4}He bath. The screwdriver is also cooled with a similar arrangement. The flange and the vacuum can are immersed in a ^{4}He bath whose temperature is electronically controlled at a temperature below the calorimeter's.

A heater with a resistance of 567.2 Ω is wrapped on the bottom of the calorimeter and cemented to it with Ge 7031 varnish. This heater is made of Manganin[21] wire and is provided with two current and two voltage leads. A germanium resistor[22] is used as the main thermometer and is fitted snugly in a hole drilled on top of the calorimeter. This resistor consists of a germanium crystal encapsulated with 1 atm of ^{4}He as exchange gas. The capsule itself is placed in good thermal contact with the calorimeter by using a film of Apiezon *N* vacuum grease.[23] All electrical connections made to the calorimeter are through superconducting niobium-zirconium wires which are thermally anchored to posts on the flange. These wires have been stripped of their copper coating except at the ends, which had to be soldered. The bare sections were electrically insulated with GE 7031 varnish. Because superconducting leads are used there are no corrections necessary for heat generation in the leads. The heater was in sufficiently good contact with the calorimeter that the leads did not warm above the superconducting transition temperature. We could not detect a dependence of the measured heat capacity upon the rate of heat input or total time of heating.

When the calorimeter is isolated by raising the screwdriver and the countertorque, the measured residual thermal conductivity to the bath was 8×10^{-7} W/K. Almost all of this is due to the stainless-steel filling capillary, with minor contributions from the electrical leads and the nylon strings. A constant heat input of about 3.5×10^{-7} W was also measured, and is probably due to radiation down the stainless-steel tubes which escaped the radiation traps. The current through the germanium resistor is an additional source of heat, which varied from about 1 to 0.1×10^{-7} W. All these heat inputs are balanced during the experiment by having the surrounding bath at a lower temperature than the calorimeter. It was found that for taking data one could keep the calorimeter at a "constant" temperature, i.e., with drifts of 10^{-9}–10^{-10} K/sec for periods of several hours. To achieve this the ^{4}He bath was regulated in a range

of ± 30 μK for the length of a whole run, i.e., 5–6 h. An auxiliary heater on the calorimeter could also be used as a fine adjustment to regulate the temperature drifts. It was wrapped around the body of the needle valve and provided heat inputs at a rate of $1.0-0.01\times10^{-7}$ W.

B. Toepler pump and gas-handling system

The samples of ^{4}He and ^{3}He-^{4}He mixtures were prepared at room temperature using the Toepler pump shown in Fig. 3. When a sample of a gas is introduced in the pump one can read its pressure and temperature. By using the precalibrated volume of the pump itself, one can then determine the amount of gas in the sample. The volume of the pump between the upper and lower calibrated burettes was measured by filling the pump with distilled water and decanting it into volumetric flasks. The volume thus measured between two fiducial marks on the lower and upper burette sections was 775.8 ± 0.3 ml. The over-all capacity of the pump including the calibrated upper and lower sections is about 900 ml.

The thermometer shown in Fig. 3 is graduated at intervals of 0.02 °C and can be read to 0.01 °C. To avoid rapid changes of temperature the Toepler pump is enclosed in a wooden box which is outlined in Fig. 3. The front of the box is closed with a panel of clear plastic. The pressure is read on a Texas Instruments precision gauge model 145. This gauge measures pressures from 0 to 1000 Torr with a claimed absolute accuracy of ± 0.05 Torr and a resolution of 0.01 Torr.

The gaseous sample of ^{4}He was taken from a storage Dewar containing liquid ^{4}He. An evacuated tube with a rubber stopper in one end led from the Dewar to the manifold. When the stoppered end of the tube was immersed in liquid ^{4}He, it began to leak. Some of the liquid ^{4}He which entered the tube through the leak was evaporated to make the gas sample. This method of obtaining a sample makes it virtually free of impurities, with the exception of the isotope ^{3}He present at a concentration of ~0.1 ppm. The ^{3}He gas used to prepare the mixtures had an isotopic composition of 99.9 at.% ^{3}He, 0.1 at.% ^{4}He, and traces (~2×10^{-10} at.%) of tritium (according to the supplier[24]).

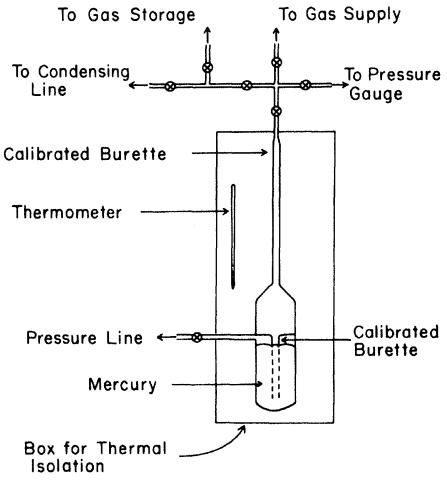

FIG. 3. Toepler pump for gas handling. This system was used to prepare the mixtures and measure the number of moles in the calorimeter.

The manifold on top of the Toepler pump shown in Fig. 3 has lines labeled "to gas storage" and "to condensing line." The former leads to a 2-l glass flask where the mixtures are stored, and the latter leads to the calorimeter. The additional line labeled "pressure line" leads to a vacuum pump or to a gas tank at pressure higher than atmospheric. Using this line, the mercury level can be raised or lowered to any desired position.

The gaseous mixtures are prepared in the following manner: A sample of ^{3}He is taken from the supply tank and put in the 2-l storage flask at a pressure P_1; ^{4}He is then introduced into the flask up to a final pressure P. If the temperature has not changed in this process then the ^{3}He mole fraction is given by $x = P_1/P$. The mole fraction of the gaseous mixture prepared this way is known to better than 0.1%. After condensing these mixtures into the calorimeter, their measured λ temperatures agreed with values from the literature[13] within the error of our temperature scale, ± 2 mK. This was a good check on the preparation of the mixture, and an indication that no fractionation of the two isotopes had occurred while condensing (which was always done above the λ temperature). For the measurements of constant-volume specific heats the condensing procedure was altered to the extent that the calorimeter was overfilled and the liquid rose about 30 cm along the condensing line, thus encountering a significant temperature gradient. A small amount of fractionation did occur in this case.

C. Electronics

The circuit to provide a measured heat input into the calorimeter consists of a power supply[25] to which a known resistor is connected in series with the heater on the calorimeter. The voltage across the resistors is measured with a differential voltmeter,[26] thus giving the power input. To obtain the total energy a timer[27] is triggered to measure the time interval when the voltage is applied. The measurements in the heating circuit never give a significant contribution to the error in the heat capacity. Typically, the error contribution from this source is 0.1–0.01 of the error contributed from the measurements of temperature intervals.

The calorimeter temperature is determined by

measuring the resistance of a germanium thermometer. The ac bridge[28] used is shown in Fig. 4. A signal from the oscillator drives the bridge through the 6:1 transformer.[29] The voltage drop across the germanium resistor is then compared through a 1:1 isolation transformer[30] with a fraction of the voltage across the standard resistor.[31] The difference between these two signals is fed to a preamplifier and a lock-in detector.[32] Its output is then displayed on a chart recorder.[33] The bridge is operated almost always near balance, and hence the ratio-transformer voltage output is nearly equal to the voltage across the germanium resistor.

For this particular bridge the frequency stability of the oscillator is important. At a frequency of 430 Hz while measuring a 5 000-Ω unknown and using a 10 000-Ω standard, we measured a frequency dependence of 0.06 Ω/Hz, corresponding to 10 μK/Hz. The amplitude stability is also important since at the power levels used (~1.0–0.1 erg/sec across the germanium resistor) the temperature of the resistor is higher than the temperature of the calorimeter. This self-heating was measured to be 300 μK/(erg/sec).

The ratio transformer has seven decades of resolution. Only six of these decades were used in the experiment, and in none of the measurements was the accuracy of the ratio transformer a limiting factor in the ultimate accuracy of the data.

All components of the bridge were carefully shielded and thermally insulated to ensure maximum stability. At the start of the experiment the stability of the bridge was checked over a period of 15 days by measuring the resistance of the germanium thermometer at the λ transition of pure ^{4}He. Although the data from day to day scattered within ± 15 μK no systematic drift was observed. At the end of the first five months of data taking, however, a shift in the λ resistance corresponding to approximately − 100 μK was measured. Five months later a similar shift was again observed. This is presumably an "aging" effect of the germanium thermometer or perhaps the standard resistors in the bridge. If this drift were uniform in time it would imply that in a typical run the λ resistance would drift by an amount corresponding to 0.1 μK. Such a drift is unimportant because it is at the limit of temperature resolution with a thermometer power level of 1 erg/sec.

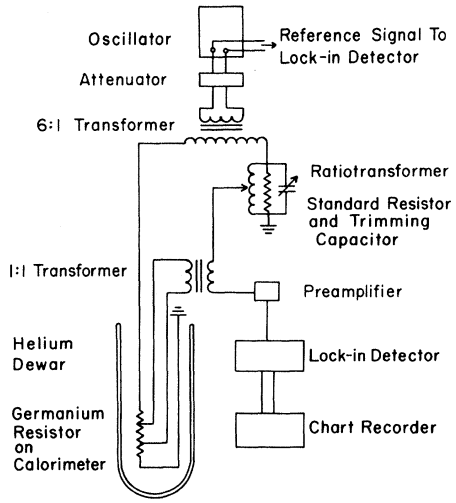

FIG. 4. Schematic of the ac resistance bridge used in conjunction with the germanium thermometer.

D. Calibration of germanium thermometer

The germanium resistor was calibrated against the vapor pressure of ^{4}He.[34] This calibration was done by having the germanium resistor in good thermal contact with the ^{4}He bath via ^{4}He exchange gas in the vacuum jacket. Simultaneous measurements of resistance and bath vapor pressure were then made. Two resistors were calibrated this way. Both resistors (identified by the manufacturer as Nos. 614 and 1019) were on the calorimeter, as indicated in Fig. 2 (only one is shown there). The resistance of No. 1019 was measured using the same dc potentiometer arrangement used in the measurements of the heating circuit. The temperature range covered was between 3.7 and 1.8 K. Subsequently, in a separate experiment,[35] this range was extended to 1 K by using the vapor pressure of liquid ^{3}He as a thermometric standard.

Thirteen data points taken this way were fitted to the function

$$\log_{10} R = \frac{1}{T} \sum_{n=0}^{N} A_n (\log_{10} R)^n , \tag{8}$$

where R is resistance and T temperature. Six coefficients provided a satisfactory fit over the whole temperature range with a scatter of less than ± 0.002 K. Resistor 1019 had been precalibrated by the manufacturer and good agreement was found between this calibration and our own. Other functions were tried in place of Eq. (8) but made no significant difference in the closeness of the fit.

It was very important for our measurements that the derivatives dR/dT and d^2R/dT^2 be accurately established as well as $R(T)$. The first derivative enters as a multiplicative factor in computing the specific heat, while the second derivative makes the major curvature contribution; i.e., the change in dR/dT with T, if not accurately measured, would contribute an extraneous temperature dependence to the specific heat. For these reasons there is an optimum number of parameters which must be used in Eq. (8) so that one does not overfit, i.e., obtain good agreement with the input data at a cost of a

very "wiggly" R versus T. We found that using five, six, seven, or eight parameters in Eq. (8) gave us good fits with dR/dT varying by ~0.4% and d^2R/dT^2 by 2%. These derivatives also agreed with those obtained using the manufacturer's calibration within the same percentage. By assuming that the variation of d^2R/dT^2 with the number of parameters used is representative of the errors in our knowledge of this derivative, we estimate a systematic error in heat capacity of 0.04% in going from T_λ to $T_\lambda \pm 0.01$ K. Similarly, the error in dR/dT implies that the absolute value of the heat capacity is uncertain by 0.4%. This latter error is irrelevant to our main objective of measuring the temperature dependence of the heat capacity.

To take data we used resistor No. 614 with the ac bridge shown in Fig. 4. When this bridge is balanced the ratio-transformer setting is not at the same ratio as one would measure with a dc bridge. This is a result of the way the capacitance and inductance across the unknown and standard resistors enter into the conditions for balance. For instance, a 5000-Ω resistor being measured by this bridge at 430 Hz and using a 10000-Ω standard would be balanced at the ratio 0.5011. For this reason, resistor No. 614, together with the ac bridge, was calibrated against the dc measurements of No. 1019 near the λ temperature of each mixture studied. Thus a secondary temperature scale was obtained at each concentration which was used for the computation of the heat capacity. Resistor No. 1019 functioned as a transfer standard from the primary vapor-pressure calibration to the working thermometer, resistor No. 614.

E. Determining volume of calorimeter

The heat capacity of interest at the λ line is C_{px} for the liquid mixture. A calorimeter which is very nearly filled with liquid will follow very closely a path of constant pressure and liquid concentration. The actual measured heat capacity has, however, contributions from the vapor phase and from the process of vaporization and condensation. To determine these contributions it is necessary to know the volume of the liquid and the volume of the calorimeter.

To determine the calorimeter volume we filled it completely with ^{4}He at about 1.4 K at a pressure just above the saturated vapor pressure. We closed the needle valve and warmed the calorimeter up to 2.5 K. In this temperature range the liquid's molar volume under its vapor pressure first decreases and then increases.[36] The helium in our calorimeter goes from a one-phase region to a two-phase and back to a one-phase region. These transitions are marked by a jump in the heat capacity given by

$$C_{\mathrm{svp}} - C_v = T \left.\frac{\partial P}{\partial T}\right|_v \left.\frac{\partial v}{\partial T}\right|_{\mathrm{svp}} . \tag{9}$$

In a typical case this jump was a few percent of the saturated-vapor-pressure specific heat (C_{svp}), thus easily observed. We readily obtained the calorimeter volume by measuring the temperature at which the jumps occur and the number of moles in the calorimeter and by using the molar volume-temperature data of Kerr and Taylor.[36]

F. Heat capacity of empty calorimeter

The heat-capacity data of the empty calorimeter were measured in the region between 4 and 1.5 K. They were then fitted to the function

$$C = AT + BT^3 . \tag{10}$$

The coefficients $A = 0.00421$ (0.00453) $\mathrm{JK^{-1}}$ and $B = 0.000312$ (0.000325) $\mathrm{JK^{-3}}$ were obtained. The set of numbers in parentheses refer to the second calorimeter heat-capacity data were fitted to Eq. (10) the scatter of the points was less than 2%. The calorimeter heat capacity was always less than 1% of its contents, and hence the errors in the measurement of the calorimeter heat capacity do not contribute significantly to the errors in measurement of the heat capacity of the helium.

G. Procedure

The samples of mixtures were condensed above their λ temperature to avoid fractionation. The amount condensed was such as to have a very nearly filled calorimeter near T_λ, thus avoiding large vaporization corrections.

After condensing the needle valve was closed, and any liquid remaining in the filling line pumped out. After this, the calorimeter was isolated by raising the mechanical heat switch (see Fig. 2).

To determine the λ temperature and plan a run, we let the calorimeter drift through the λ transition and observed the temperature on the chart recorder. With constant heat input the slope of the trace on the chart recorder is a measure of the reciprocal of the heat capacity. A sudden change of slope in a very narrow temperature region is the indication of the λ temperature. Having identified this temperature, the taking of data is planned so that one converges on the transition using successively decreasing temperature intervals. Typically, four to seven data points are taken for each temperature decade away from T_λ. The temperature resolution limits the data severely in the 10^{-5}–10^{-6} decade; for this reason temperature intervals smaller than about 3×10^{-6} K were never used. Often when several runs were made on a particular sample, the size of the interval used in a particular decade was varied and no dependence of the heat capacity upon this interval size was observed.

Data were taken by observing the drift for several minutes, heating for a time interval of about 1 min or longer, and then observing the drift again.

TABLE II. Results of fitting the data for C_{px} to the power-law expression, Eq. (12).

x	α'	A' (J mole^{-1} K^{-1})	B' (J mole^{-1} K^{-1})
0.0000	−0.012 026 ± 0.0036	5.717 ± 0.15	12.791 ± 0.56
0.0110	−0.033 70 ± 0.01	6.318 ± 0.44	10.229 ± 1.61
0.0997	−0.093 94 ± 0.0038	6.046 ± 0.14	8.684 ± 0.48
0.200	−0.1559 ± 0.0081	4.991 ± 0.20	8.428 ± 0.72
0.301	−0.1713 ± 0.0078	2.761 ± 0.11	10.714 ± 0.39
0.390	−0.1717 ± 0.0129	1.446 ± 0.084	10.794 ± 0.30
0.530[a]	−0.2773	0.593	8.959
	α	A (J mole^{-1} K^{-1})	B (J mole^{-1} K^{-1})
0.0000	+0.012 458 ± 0.0028	4.923 ± 0.10	−6.256 ± 0.38
0.0110	+0.016 19 ± 0.0083	4.655 ± 0.28	−5.209 ± 0.48
0.0997	−0.033 67 ± 0.0037	4.892 ± 0.13	−4.351 ± 1.0
0.200	−0.0891 ± 0.0054	4.531 ± 0.15	−1.617 ± 0.44
0.301	−0.1584 ± 0.0044	4.423 ± 0.10	−0.585 ± 0.55
0.390	−0.2047 ± 0.0046	3.194 ± 0.072	+2.872 ± 0.25
0.530[a]	−0.3053	2.649	+2.755

[a]Data from T. A. Alvesalo, P. M. Berglund, S. T. Islander, G. R. Pickett, and W. Zimmermann, Jr., Phys. Rev. A 4, 2354 (1971); W. Zimmermann, Jr. (private communication).

The total temperature change for a data point can then easily be inferred from the bridge readings and the drifts extrapolated to the middle of the heating interval. The temperature drift of the calorimeter could be adjusted to between 10^{-9} and 10^{-10} K/sec by heating with the auxiliary heater and germanium thermometer while simultaneously regulating the helium bath at about 1.3 K to provide a negative heat input.

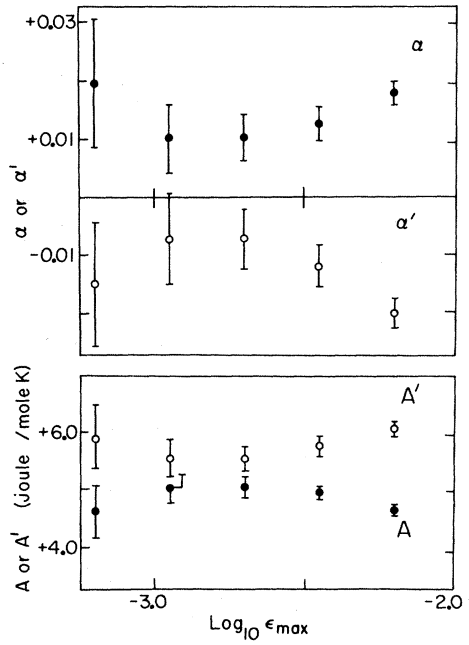

FIG. 5. Power-law parameters α, α', A, and A' for pure ^{4}He as a function of the maximum range of data away from T_λ used in the computer fit.

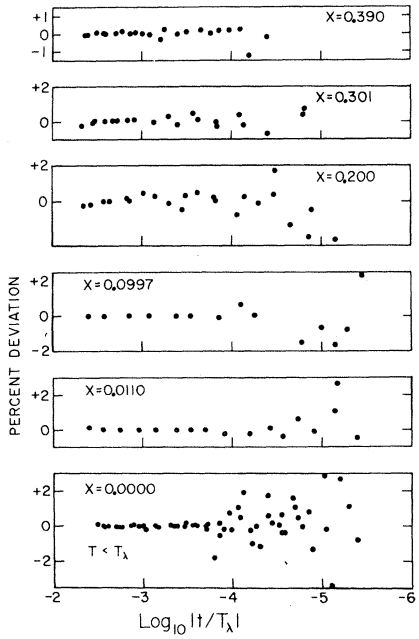

FIG. 6. Percent deviation of the specific heat at constant mole fraction for $T < T_\lambda$ when fitted to a power-law temperature dependence, Eq. (12). Data for temperatures farther from T_λ than those shown here deviated systematically from the fitted function.

Upon completing a successful run, the mixture was removed from the calorimeter and measured with the Toepler pump.

IV. DATA AND DATA ANALYSIS

We have made 165 separate specific-heat measurements on pure ^{4}He and 433 measurements on ^{3}He-^{4}He mixtures. The raw data are available from one of the authors (FMG) and are tabulated in Ref. 37. Here we have chosen to present the derived specific heat, C_{px}. This specific heat is of greater physical interest and only slightly removed from the raw data in the range $|T - T_\lambda| < 0.01$ K. A quantitative representation of C_{px} is given by the power law, Eq. (12), together with the λ-line parameters listed in Table I and the coefficients and exponents listed in Table II (and graphed in Fig. 5). The precision with which the power law represents the data is evident from the graphs of deviations shown in Figs. 6 and 7. The qualitative features of C_{px} are evident in Figs. 1, 8, and 9.

This section is divided into two subsections, one dealing with pure ^{4}He and the other with ^{3}He-^{4}He mixtures. In each subsection we first concern ourselves with the relationship between the measured specific heat, C_m, and the specific heat C_{px} (or C_p in the case of pure ^{4}He). We then describe the procedures we have used to obtain algebraic representations for these specific heats for further use. Section V is concerned with the implications of our

data in terms of "scaling," "renormalization," and "universality."

A. Data on ^{4}He

1. *Obtaining* C_p. The specific heat measured in our experiment is very nearly C_p. The measurements contain contributions from the calorimeter, the vapor in equilibrium with the liquid, and from the process of vaporization. In addition, the liquid follows a path in temperature along the coexistence curve which is not at constant pressure. The contribution from the calorimeter is readily subtracted. This leaves a specific heat which we call C_m. Corrections from the vapor and vaporization can be made using the formula

$$\frac{(1/n_l)C_m - C_p}{T} = -\frac{\partial v_l}{\partial T}\bigg|_p \frac{dp}{dT} - \frac{s_l - s_v}{n_l} + \frac{n - n_l}{n_l}\frac{ds_v}{dT}\,, \tag{11}$$

which involves the first three terms of the more general equation derived in the Appendix for the case of mixtures. (Here n_l is the number of moles in the liquid phase, s_l is the molar entropy of the liquid phase, etc.) Equation (11) was first derived in Ref. 38 and is a special case of a more general equation derived in Ref. 6. Although the first term on the right-hand side of this equation has the same singularity as C_p, it is small in magnitude. The other two terms are small in virtue of the high

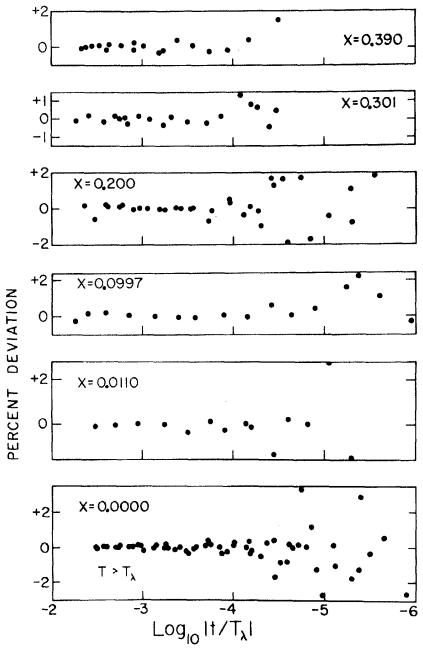

FIG. 7. Percent deviation of the specific heat at constant mole fraction for $T > T_\lambda$ when fitted to a power-law temperature dependence, Eq. (12). Data for temperatures farther from T_λ than those shown here deviated systematically from the fitted function.

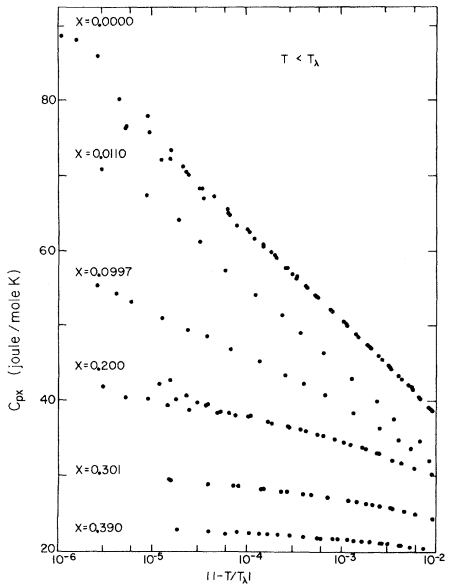

FIG. 8. Specific heat at constant mole fraction for $T < T_\lambda$. The λ temperature for this graph was chosen by a least-squares-fitting procedure to the power-law temperature dependence, Eq. (12). For clarity the data at $x = 0.0110$ have been shifted down 5 J/mole K while the data at the three highest mole fractions have been moved up the same amount.

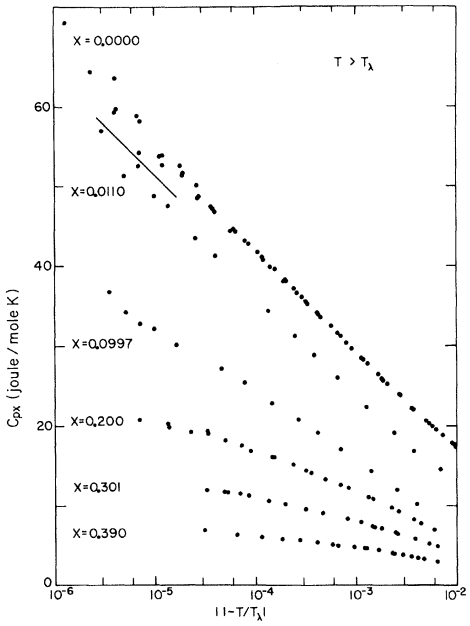

FIG. 9. Specific heat at constant mole fraction for $T > T_\lambda$. The λ temperature for this graph was chosen by a least-squares-fitting procedure to the power-law temperature dependence, Eq. (12). For clarity the data at $x = 0.0110$ have been shifted down 5 J/mole K, while the data at the other four mole fractions have been shifted down 10 J/mole K.

liquid-filling fraction. The total contribution of the right-hand side of Eq. (11) varied between 0.02 and 0.2% of C_m in the region where the data were analyzed. These corrections were used prior to further analysis. The correction of the data from C_p along the coexistence path to C_p along the path $P = P_\lambda$ is less than 0.01% and hence totally negligible.

(2) *Fitting data.* Our early interest in pure ^{4}He was simply to provide a control experiment for the measurements on the mixtures. These data, however, showed an interesting asymmetry between the branches above and below T_λ, indicating that the conclusion of a symmetric, i.e., equal, amplitude logarithmic divergence from the data of Ref. 1 was not correct. Shortly after our measurements Ahlers published his own data on ^{4}He at saturated vapor pressure[11] and later at higher pressures.[39] He has discussed these data and their implication to scaling and universality. We have fitted our data to the function

$$C_p = (A/\alpha)(\epsilon^{-\alpha} - 1) + B , \tag{12}$$

where $\epsilon \equiv t/T_\lambda$ and the parameters A, α, B were allowed to take different values above and below T_λ. In the latter case, as has become customary, we denote these parameters by primes. The λ temperature itself was treated as a variational parameter. As an alternative to Eq. (12) we tried explicitly to have both α and α' zero using the form

$$C_p = -A \ln\epsilon + B . \tag{13}$$

If, as $\epsilon \to 0$, the specific heat has the functional form of Eq. (12), scaling predicts $\alpha = \alpha'$. If the specific heat has the functional form of Eq. (13), scaling predicts [40,41] $A = A'$. In the computer analysis we actually used the integrals of Eq. (12) or (13) and compared them with the heat added to span a given temperature interval. Using this procedure one avoids curvature corrections associated with the assignment of a temperature (usually the middle of the heating interval) to a heat-capacity point. There were no gravitational corrections made to the data. These corrections would be negligible except for data which spanned the transition, and in some cases with calorimeter (1), a data point on either side of T_λ. These points were omitted from the analysis. To fit the data to Eqs. (12) and (13), we weighted each point according to the expected random error in the heat capacity, which is 0.1% for temperature intervals $\Delta T \geq 10^{-4}$ K and grows progressively larger for smaller intervals due to the temperature resolution of about 10^{-7} K. The weights were

$$w = \left(\frac{1}{0.001 C_p}\right)^2 \qquad \text{for } \Delta T > 10^{-4} ,$$

$$w = \left(\frac{1}{0.001 C_p + 10^{-7} C_p/\Delta T}\right)^2 \qquad \text{for } \Delta T < 10^{-4} . \tag{14}$$

We used a standard error analysis[42] to determine the variance in the parameters in Eqs. (12) and (13), with the exception that we expanded Eq. (12) for α small and used

$$C_p \cong b_1 + b_2 \ln\epsilon + b_3 (\ln\epsilon)^2 , \tag{15}$$

where $b_1 = B$, $b_2 = -A$, and $b_3 = \frac{1}{2} A\alpha$. Also, in this calculation of the variance we took T_λ as fixed, while in fact it is a variational parameter. We made several different numerical experiments to assure ourselves that the error in this approximation for computing the variance in α, A, B and α', A', B' is not serious. The variances of b_1, b_2, and b_3 in Eq. (15) are given as the diagonal elements of the error matrix, which is the reciprocal of the matrix whose elements are

$$\alpha_{ij} = \sum_{k=1}^{N} w_k (\ln\epsilon_k)^{i-1} (\ln\epsilon_k)^{j-1} , \tag{16}$$

where $i, j = 1, 2, 3$ refer to subscripts of the b's in Eq. (15) and k runs over N data points.

Four sets of data on ^{4}He were fitted simultaneously to Eq. (12). A total of 10 parameters were varied to achieve an optimum fit. They were T_λ for each of the four sets, α, α', A, A', B and B'. In Fig. 5 we show the values of the parameters α, A, α' and A' as a function of the range of data, ϵ_{max}, used in the fit. Thus the point in Fig. 5 at $\epsilon_{max} = 10^{-3}$ means that only data in the range $0 < \epsilon \leq 10^{-3}$ are used. A decade of ϵ_{max} from 6×10^{-3} to 6×10^{-4} was explored this way. The number of data points included for $\log_{10}\epsilon_{max} = 2.2$ and -3.2 was 132 and 91, respectively, decreasing by about 10 at each successive value of ϵ_{max}. At $\log_{10}\epsilon_{max} = -2.2$ the deviation of the data from Eq. (12) is systematic; for $\log_{10}\epsilon_{max} \leq -2.45$ Eq. (12) fits the data well. Although the variations in the parameters in Fig. 5 seem to indicate a slight range dependence for $\log_{10}\epsilon_{max} \leq -2.45$, we note that these variations are all within the expected error, as computed from the error matrix. The results for $\epsilon_{max} = -2.45$ are listed in Table II and the deviation of the data from the fitted function for $\epsilon_{max} = -2.45$ is shown in Figs. 6 and 7. It can be seen from this figure that Eq. (12) fits the data well with no evidence of systematic deviations.

In every case we studied, we found that the variation of the "best-fit" T_λ as a function of ϵ_{max} amounted to less than $\pm 3\times10^{-7}$ K. This confirmed our assumption that the data determine T_λ with great precision.

B. Data on mixtures

1. *Obtaining C_{px}.* Before proceeding with a more detailed analysis we have to verify how close

our measured specific heat is to C_{px}. As in the case of ^{4}He, our measurements were done in a partly filled cell following a path of liquid and vapor coexistence. The same considerations outlined for ^{4}He to obtain C_p apply here to obtain C_{px}. In addition, the fact that the ^{3}He concentrations in the liquid and vapor differ introduces the additional variable of concentration. The following equation, derived in the Appendix, gives the difference between C_m and C_{px},

$$\frac{(1/n_l)C_m - C_{px}}{T} = -\frac{\partial v_l}{\partial T}\bigg|_{p,x_l}\frac{dP}{dT} - \frac{s_l - s_v}{n_l}\frac{dn_l}{dT} + \frac{n - n_l}{n_l}\frac{ds_v}{dT} - \left[\frac{\partial \phi}{\partial T}\bigg|_{p,x_l} + \frac{\partial \phi}{\partial p}\bigg|_{x_l,t}\frac{dP}{dT} - \frac{1}{x_l - x_v} \times \left((v_l - v_v)\frac{dP}{dT} - s_l + s_v\right)\right]\frac{\partial x_l}{\partial T}\bigg|_{p,\phi} . \quad (17)$$

The particular form of this equation is useful in converting C_m to C_{px} insofar as it isolates a possibly singular term, i.e., $(\partial x_l/\partial T)|_{p,\phi}$. This partial derivative can be related to $C_{p\phi}$ as in Eq. (7), and if $C_{p\phi}$ diverges at T_λ so does $(\partial x_l/\partial T)|_{p,\phi}$. We discovered however, that Eq. (17) is not very useful if one wants to calculate $C_m - C_{px}$ using presently available data. The coefficient of $(\partial x_l/\partial T)|_{p,\phi}$ involves the difference of large numbers and is hard to evaluate accurately. A simpler form of Eq. (17) which avoids this difficulty but which smoothes out the possible singularity of the last term was used to estimate $C_m - C_{px}$. This is Eq. (A12) of the Appendix. It was found that where this latter equation is expected to be valid, $\epsilon \sim 10^{-2}$, $C_m - C_{px}$ was less than 0.1% for all cases except at $x = 0.200$. In this case the difference was approximately +0.2 and +0.4% for temperatures 0.02 K greater and less than T_λ, respectively.

Although reassuring, the estimate using Eq. (A12) is not totally convincing, since it does not properly take into account the possibly singular term $(\partial x_l/\partial T)|_{p,\phi}$. The contribution of this term is independent of the filling fraction and hence cannot be minimized by having a nearly filled cell. To see how close C_m is to C_{px} for the data closer to T_λ we decided to carry out a further check at $x = 0.30$ by measuring C_{vx}. At this mole fraction it can be easily checked that at a molar volume sufficiently close to the saturated-vapor-pressure molar volume $(C_{px} - C_{vx})/C_{px} \leq 0.1\%$. Hence, if C_m is measured at the same average liquid mole fraction as C_{vx} and if the two are found to coincide, then one can conclude that C_m is essentially equal to C_{px}. The result of these measurements is shown in Fig. 10. Here we show three sets of data: two at constant volume and one with a 99% filled cell. The mole-fraction label on these latter data refers strictly to the average of liquid and vapor rather than to the liquid alone. The data in Fig. 10 were intended to be at the same mole fraction; however, a measurable fractionation of the liquid occurred when the samples were condensed in the calorimeter. As we mentioned in Sec. III, the filling procedure for the measurements of C_{vx} was different than for C_m. To achieve the original goal of showing $C_m \cong C_{px}$, we calculated the value of C_m at the concentration of C_{vx} and corrected C_{vx} to the average saturated-vapor-pressure molar volume. We carried this calculation[43] out for both sets of C_{vx} data. Our conclusions are that at $x = 0.30$, $|C_{vx} - C_m| \leq 0.002\ C_m$ for the whole temperature region which will be used for data analysis, i.e., $\epsilon < 4.5 \times 10^{-3}$.

One can extend now this conclusion to the other mixtures. We have already shown that farther away from T_λ, $|C_m - C_{px}| < 0.001\ C_{px}$, except for $x = 0.20$, where this difference is a bit larger. Now we have established that at $x = 0.30$ the temperature dependence of this difference in the region closer to T_λ is also small. This temperature dependence comes from the filling independent term $(\partial x_l/\partial T)|_{p,\phi}$, which is weakly dependent on x in the sense that its temperature dependence near T_λ is very nearly the same at all mole fractions. Under these circumstances, then, our conclusion that $C_{px} \cong C_m$ at $x = 0.30$ holds for all the other mixtures we studied.

2. *Data analysis.* In Figs. 8 and 9 we have plotted our data as a function of $(T - T_\lambda)/T_\lambda$. Note the data have been displaced vertically in the figures, as indicated in the captions. The data for all the mixtures were fitted in the same fashion as for pure ^{4}He; i.e., the energy per mole required to

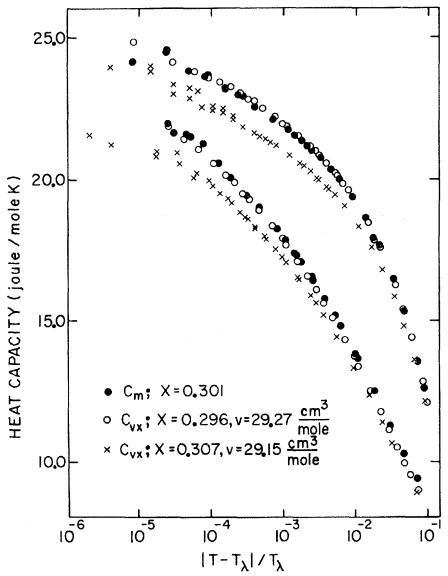

FIG. 10. Data for C_{vx} and C_m in the neighborhood of $x = 0.30$. Here $C_m \cong C_{px}$.

span a temperature interval was tested to the integrated form of Eq. (12). The errors in the best-fit parameters were also generated using the same procedure as for pure ^{4}He. The maximum range of data which could be used was $\epsilon \lesssim 4.5\times10^{-3}$. Outside this range the data deviated systematically from Eq. (12). The results for the variational parameters are listed in Table II. In Table II we also give the results of the same analysis for the data at $x = 0.53$ from Ref. 6. In Figs. 11–13 we have plotted the parameters α, α', A, A', B, B' as a function of mole fraction. We see from these figures that the parameters are smooth functions of mole fraction. In particular, as observed in the case of pure ^{4}He, α seems to remain larger than α', at least up to $x \cong 0.35$. The parameters A and A' can be smoothly extrapolated to zero at the tricritical point ($x = 0.68$), while B and B' take the value near 8 J/mol K there. This seems to be consistent with the measurements near the tricritical point.[6] The solid lines in Figs. 11–13 have no particular significance and have been drawn to aid the eye.

The increasingly negative values of α and α' (as x is increased) are quantitative representations of the renormalization effects visible in Figs. 1, 8, and 9: As one moves to higher mole fractions the specific heat loses most of its temperature dependence and shows progressively greater negative curvature. We have discussed this feature of the data in an earlier publication.[5] We find no evidence that the specific heat has a jump at T_λ, as has been thought. Indeed, the difference between the branches above and below the transition goes to zero increasingly rapidly as one approaches the transition. It also becomes apparent, especially at the higher concentrations, that C_{px} is finite, as is required by thermodynamics. The derivative of C_{px} with respect to temperature is divergent whether calculated numerically from the data themselves, as we did in Ref. 5, or from Eq. (12) with α and α' negative.. Thus C_{px} reaches finite values at T_λ with infinite slope. The same conclusions have also been reached for data at higher mole fractions by Alvesalo *et al.*[6]

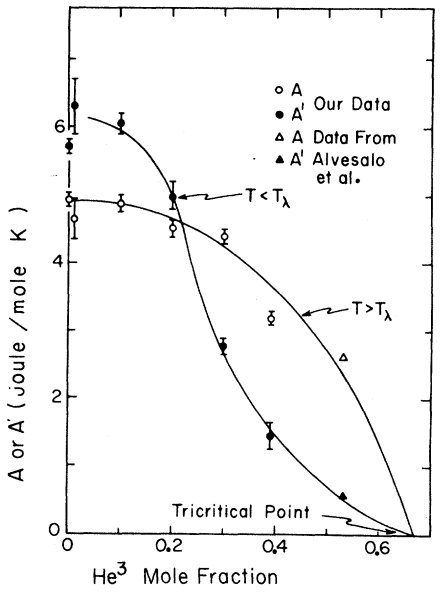

FIG. 12. Parameters A and A' in the power-law dependence of C_{px} as a function of He^3 mole fraction.

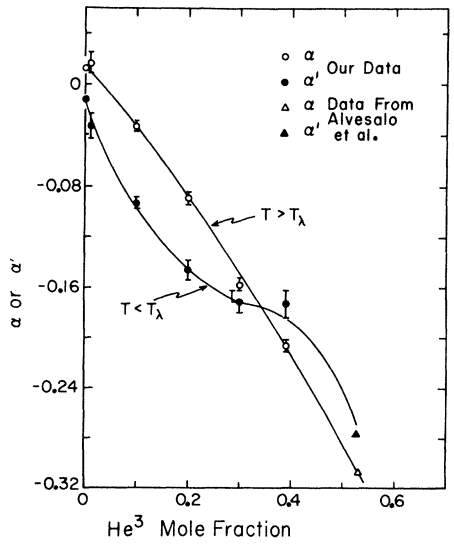

FIG. 11. Exponents α and α' of the power-law dependence of C_{px} as a function of ^{3}He mole fraction.

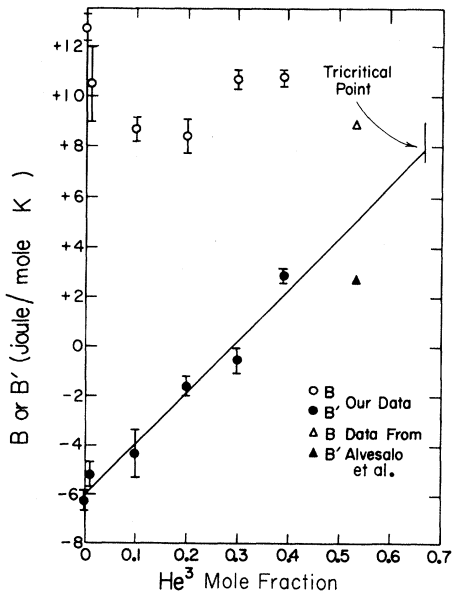

FIG. 13. Parameters B and B' in the power-law dependence of C_{px} as a function of ^{3}He mole fraction.

V. SCALING AND UNIVERSALITY

We will now consider our data from the point of view of scaling and universality. For this purpose we assume that pure ^{4}He is an "ideal" system for which C_p (along a path of constant pressure) may exhibit a nonanalytic possibly divergent temperature dependence at T_λ characterized by the exponents α and α' [Eq. (12)]. We will find that the scaling prediction $\alpha = \alpha'$ is not satisfied unless one presumes that singular correction terms to Eq. (12) exist. Until we have more theoretical guidance to the form of such terms, data with the precision and closeness of approach to T_λ of our own cannot determine a value of α consistent with scaling. In order to examine the data for the ^{3}He-^{4}He mixtures from the viewpoint of universality, we must first compute $C_{p\phi}$ along paths of constant ϕ. We will then find that the data are consistent with the universality prediction that $C_{p\phi}$ has the same temperature dependence near T_λ [Eq. (12) with the same values of α and α'] as does C_p in pure ^{4}He. Thus the data on mixtures provide an independent indication of the need for singular correction terms to scaling. This is particularly important because the mixture data are subject to quite different systematic errors than are the data on pure ^{4}He (for example, the superfluid mixtures do not have an effectively infinite thermal conductivity, as does superfluid ^{4}He). Unfortunately, the values of α and α' for $C_{p\phi}$ in the mixtures with larger values of x are subject to greater errors than are the corresponding exponents for pure ^{4}He. This occurs because some of the thermodynamic quantities which are needed to convert C_{px} to $C_{p\phi}$ [particularly $(\partial s/\partial T)|_{p,\lambda}$] are not well known for these mixtures.

From the point of view of universality, the finite and cusped character of C_{px} and C_m in the mixture is the almost trivial result of our choice of thermodynamic path for the measurements and our measurement of the specific heat at constant x (which cannot diverge along the λ line) rather than at constant ϕ. Nevertheless, we feel a remark reemphasizing these qualitative features is appropriate. There are few pure laboratory systems with λ-like phase transitions which are known to remain sharp at the $\epsilon = 10^{-5}$ level when the pure system is diluted by 40% with an impurity which reduces the transition temperature by one-third. Most solid systems with even small impurity concentrations have macroscopic inhomogeneities which cannot equilibrate on the time scale of laboratory experiments; hence their λ-like phase transitions become "rounded." Experiments near the critical point of pure fluid systems indicate rounding from gravitationally induced density gradients at this level, and it is likely that experiments on binary fluid systems will also be subject to such effects.[44] Thus in some respects helium mixtures are an ideal experimental system in which to study scaling and universality.

Upon applying the procedures we described in Sec. V to the data for pure ^{4}He, we obtained for the constant-pressure specific heat the exponents $\alpha = 0.0125 \pm 0.0028$ and $\alpha' = -0.0120 \pm 0.0036$. These exponents disagree with the prediction from scaling that they should be equal. In particular, the branch for $T < T_\lambda$ seems to tend to a finite value, while $T > T_\lambda$ diverges. A similar asymmetry when using Eq. (12) was found by Ahlers.[11] His exponents are $\alpha = 0.000 \pm 0.003$ and $\alpha' = -0.020 \pm 0.003$. The differences between our exponents and Ahlers's equal four times and twice the sum of the standard deviations for α and α', respectively. The explanation of this difference is not clear.

A subset of the data we used for the power-law fit was also tested explicitly by setting $\alpha = \alpha' = 0$, i.e., with Eq. (13). In these fits the deviation of the data from the Eq. (13) was *always systematic* when the range of $\log_{10}\epsilon_{max}$ was changed from -2.2 to -3.2. It was found that A/A' varied monotonically from 1.04 to 1.08 in the same range. We conclude that, if one is willing to further limit the range of data so that the systematic deviations from Eq. (13) are within the random error of these data, then $A > A'$. This is again a result which disagrees with scaling.

One could extend the above analysis to further investigate the seriousness of the discrepancy with scaling by forcing $\alpha = \alpha'$ and compensate for this constraint by adding singular higher-order terms of Eq. (12). Or, alternatively, one could add higher-order terms to Eq. (13) with the constraint $A = A'$. Ahlers has tested a number of alternatives along these lines against his data (which have a precision comparable to our own in pure ^{4}He) and was not able to reach a unique conclusion when using only his data near saturated vapor pressure. Current theory does not specify enough of the parameters in possible correction terms to make a meaningful test at this time. Thus we can only make the qualitative conclusion that imposing the constraint that the data in pure ^{4}He agree with scaling would imply a substantial contribution from these correction terms even for the data closest to T_λ. Indeed, in the particular case of Eq. (13), the smaller ϵ_{max} the larger the contribution from these terms would have to be.

We now turn to the data on mixtures and ask the question: Are they consistent with universality? A naive way of answering this question would be to compare the exponents α for C_{px} in Fig. 11 with the prediction that they be something like the fully renormalized exponent $[\alpha/(1-\alpha)]$. We would expect this renormalized exponent to be -0.01 ($\alpha = +0.01$ in pure ^{4}He), which strongly contrasts with the exponent -0.3 we obtained for C_{px} at $x = 0.39$. In fact,

we regard the value $\alpha = -0.3$ as an "effective" exponent which fortuitously describes our data in the range $10^{-5} < \epsilon < 4.5 \times 10^{-3}$. This is an illustration of our conclusion from thermodynamic arguments that a weak divergence in $C_{p\phi}$ will lead to a very slow approach of C_{px} to its maximum value, C_{max}. Thus to test universality a more laborious process is necessary. We will compute $C_{p\phi}$ from our data and compare it to C_p in pure ^{4}He. Universality leads us to expect $C_{p\phi}$ to have the same exponents[45] as C_p in the same ranges of temperature away from T_λ.

In order to obtain $C_{p\phi}$ from our data the first step is to calculate $C^x_{p\phi}$ along paths of constant x via Eq. (3) and our estimate of the λ-line parameters. This specific heat along the path $x = \text{const}$ is also asymptotically divergent if $C_{p\phi}$ is; as a matter of fact, one can readily show that asymptotically $C^x_{p\phi} \sim t^{-\alpha/(1-\alpha)}$. Hence its characteristic exponent differs only by approximately 1% from $C_{p\phi}$ in an appropriate region close to T_λ. In using Eq. (3) to calculate $C^x_{p\phi}$ the λ-line parameters were assumed to have no t dependence in the range up to $t \leq 4.5 \times 10^{-3} T_\lambda$. The calculated specific heat was then fitted to Eq. (12) to obtain its characteristic exponents. These are plotted as the filled and open circles in Fig. 14 as a function of mole fraction. The rather large error bars associated with these results stem almost entirely from the uncertainty in the λ parameters. There is only a small contribution from the errors in our own data. We explored the effects of our poor knowledge of the λ parameters by setting them equal to their extreme values consistent with our error estimates (see Table I), and reevaluating $C^x_{p\phi}$. Refitting $C^x_{p\phi}$ then yields values of the exponents within the error bars of Fig. 14. This procedure could not be followed at $x = 0.53$, where the uncertainty in the λ parameters is so large that C_{max} calculated from Eq. (6) could assume values less than the largest value of the measured specific heat. Thus we expect that the uncertainty in α and α' will be even larger than at $x = 0.53$.

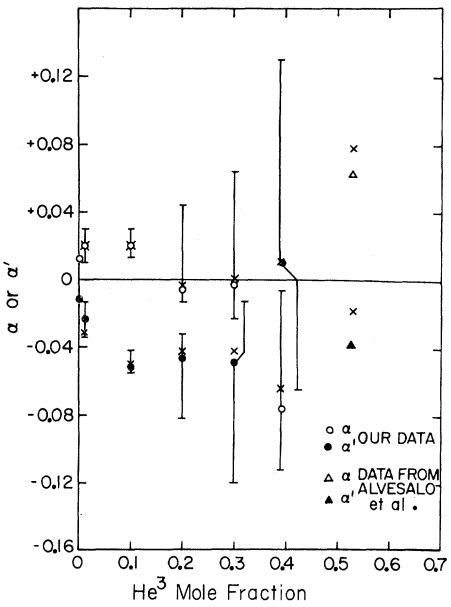

FIG. 14. Parameters α and α' in the power-law dependence of $C_{p\phi}$ along paths of constant mole fraction and along paths of constant ϕ. The ×'s refer to $C_{p\phi}$, while the other symbols refer to $C^x_{p\phi}$.

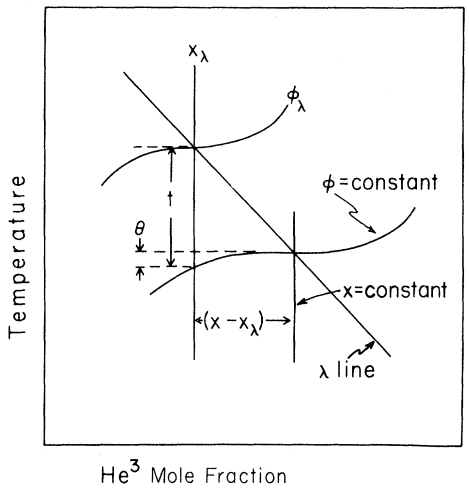

FIG. 15. Geometry in x-T space of going from a path of constant x to a path of constant ϕ.

It is clear when one compares Fig. 14 with Fig. 11 that the exponents for $C^x_{p\phi}$ do not become progressively more negative as do those for C_{px}, but rather tend to cluster closer to zero, and in particular to the values of ^{4}He. This is as expected. Before making any conclusions however, we proceed in our calculation of $C_{p\phi}$. All we have left to do is to carry out a conversion of the distance to T_λ from a path of constant x to that of a path of constant ϕ. The geometry in T-x space to carry out this conversion is shown in Fig. 15. Our experimental path is a path of nearly constant mole fraction $x = x_\lambda$. At a particular temperature we have indicated the distance $t = |T - T_\lambda(x,p)|$ along this path and the distance $\theta = |T - T_\lambda(\phi,p)|$ along a path $\phi = \text{const}$. Calculating $C^x_{p\phi}(t)$ involves using Eq. (3) without changing the distance t to θ. If we make this correction we then obtain $C_{p\phi}$ along $\phi = \text{const}$; however, if we carry this out at a series of temperatures T_1, T_2, ..., we obtain $C_{p\phi_1}(\theta_1)$, $C_{p\phi_2}(\theta_2)$..., while we want $C_{p\phi_\lambda}(\theta_1)$, $C_{p\phi_\lambda}(\theta_2)$, etc. The variations in ϕ, however, in the neighborhood of interest are small and can for all practical purposes be ignored. This we have checked explicitly by subsequently evaluating $(\partial C_{p\phi}/\partial\phi)|_\phi \delta\phi$, where $\delta\phi$ is the maximum variation in ϕ corresponding to the maximum range in θ used. We have calcu-

lated $C_{p\phi}$ using data only for $\theta < 10^{-3}\,T_\lambda$ and we found that $C_{p\phi}$ varied from its value along ϕ_λ to its value along $\phi = \text{const}$ at the extreme of the temperature range by at most about 1% at the highest mole fraction, $x = 0.53$, and less than 0.5% for all other mole fractions. Even these small deviations refer to a few data points at the extreme of the range. For the rest of the data this path effect is much less, decreasing proportionately to θ as one gets closer to T_λ.

In proceeding with the calculation of θ we are handicapped by the lack of any other thermodynamic data sufficiently close to T_λ. We thus used an iterative procedure whereby we assumed $C^x_{p\phi}(t) = C_{p\phi}(\theta)$, calculated a θ, refitted $C_{p\phi}(\theta)$ to Eq. (12), and repeated this process until it converged. In detail, we used the following procedure: We see from Fig. 15 that if we assume the λ line to be locally linear, we have (in the case of $T < T_\lambda$)

$$t = \theta - (x - x_\lambda)\left.\frac{\partial T}{\partial x}\right|_{p,\lambda}. \tag{18}$$

Further, we can integrate Eq. (7) along $\phi = \text{const}$ by assuming the λ derivatives to have no t dependence, and obtain

$$x - x_\lambda = \theta \left.\frac{\partial T}{\partial \phi}\right|_{p,\lambda}\left\{\left.\frac{\partial s}{\partial T}\right|_{p,\lambda} - \frac{1}{T_\lambda}\left[\frac{A'}{\alpha'}\left(\frac{1}{1-\alpha'}\,\theta^{-\alpha'} - 1\right) + B'\right]\right\}, \tag{19}$$

where the parameters α', A', B' refer to $C_{p\phi}(\theta)$, which has been assumed to have a power-law dependence on θ as in Eq. (12). In obtaining Eq. (19) we have also ignored the x dependence of the right-hand side of Eq. (7). This is a good approximation since at any given mole fraction we are only considering a range of $|x - x_\lambda| < 10^{-3}$. The λ parameters at all mole fractions except 0.53 differ at the extreme of this range from their value at T_λ by less than 1%, and typically a few tenths of a percent. At $x = 0.53$ this difference reaches approximately 2%. These differences are at the extreme of the mole fraction range and decrease very rapidly, in proportion to $|x - x_\lambda|$, for the data closer to T_λ.

TABLE III. Results of fitting the calculated $C_{p\phi}$ to the power-law expression, Eq. (12).

x_λ	α'	A' (J mole^{-1} K^{-1})	B' (J mole^{-1} K^{-1})
0.0000	−0.012 026	5.717	12.791
0.0110	−0.033 56	7.021	10.681
0.0997	−0.050 02	10.782	10.670
0.200	−0.042 73	10.690	10.875
0.301	−0.042 13	9.805	6.496
0.390	+0.012 44	4.666	16.970
0.530[a]	−0.018 07	13.850	−16.012
	α	A (J mole^{-1} K^{-1})	B (J mole^{-1} K^{-1})
0.0000	+0.012 458	4.923	−6.256
0.0110	+0.021 62	4.858	−4.464
0.0997	+0.020 17	6.388	−2.517
0.200	−0.003 166	7.800	−7.240
0.301	+0.001 111	7.230	−8.229
0.390	−0.064 20	8.221	−12.446
0.530[a]	+0.077 96	6.143	−16.478

[a]Data from T. A. Alvesalo, P. M. Berglund, S. T. Islander, G. R. Pickett, and W. Zimmermann, Jr., Phys. Rev. A 4, 2354 (1971); W. Zimmermann, Jr. (private communication).

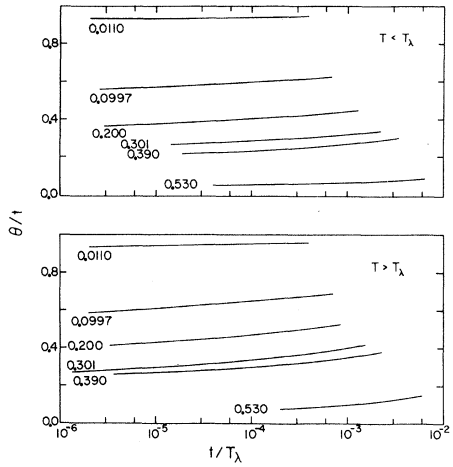

FIG. 16. Ratio of the distance to the λ temperature along a path of constant ϕ to that along a path of constant x for $T < T_\lambda$ and $T > T_\lambda$.

Combining Eqs. (18) and (19), one has

$$\theta = t\left(1 - \left.\frac{\partial T}{\partial x}\right|_{p,\lambda}\left.\frac{\partial T}{\partial \phi}\right|_{p,\lambda}\left\{\left.\frac{\partial s}{\partial T}\right|_{p,\lambda} - \frac{1}{T_\lambda}\left[\frac{A'}{\alpha'}\left(\frac{1}{1-\alpha'}\,\theta^{-\alpha'} - 1\right) + B'\right]\right\}\right)^{-1}. \tag{20}$$

This, with the identical expression for $T > T_\lambda$, is our working equation. We start our iterative process to evaluate θ by taking α', A', B', to be the parameters of $C^x_{p\phi}$. This yields the first set of θ's, θ_1's. We then fit $C_{p\phi}(\theta_1)$ to Eq. (12) to obtain a new set of α', A', B' which then go in Eq. (20) to generate a new set of θ's, θ_2's. This procedure converged after at most six iterations, after which no changes in the parameters of $C_{p\phi}$ were obtained. We have listed these parameters in Table III. In Fig. 16 we have plotted the ratio θ/t below and above T_λ.[46] It can be seen from this figure that although θ gets to be considerably smaller than t, it shows a very small t dependence. This implies that the characteristic exponents for $C_{p\phi}$ will not differ much from those of $C^x_{p\phi}$, since in the limit that θ/t is a constant these exponents are identical. This is verified in Fig. 14, in which we have plotted as ×'s the exponents for $C_{p\phi}$. The error bars for the $C^x_{p\phi}$ exponents can also be applied to the ones

for $C_{p\phi}$, since the additional step in calculating $C_{p\phi}$, the t-to-θ conversion, gives a relatively small error contribution to the exponents.

It is clear from Fig. 14, as remarked earlier in the case of $C^x_{p\phi}$, that the exponents for $C_{p\phi}$ are close to the exponents of pure ^{4}He, although perhaps not identically the same. This agrees qualitatively with the ideas of universality,[45] which predicts they should be the same. According to these ideas one expects that these exponents not be affected by the presence of ^{3}He. The similarity between $C_{p\phi}$ and C_p in pure ^{4}He is also evident in Fig. 17, where we have plotted $C_{p\phi}$ as a function of θ/T_λ. All the data seem to fall on nearly straight lines, indicating α and α' to be near zero. Indeed, except at $x = 0.53$, where the estimate of the λ parameters is especially crucial, these lines are nearly parallel. Figure 17, which shows $C_{p\phi}$, should be contrasted with Figs. 8 and 9, which show the renormalization effect for C_{px}.

A close look at Figs. 14 and 17 or Table III reveals that the same asymmetry for the exponents above and below T_λ which we observed for pure ^{4}He, persists for the mixtures. The branch for $T > T_\lambda$ has more positive exponent, except at $x = 0.39$ than the branch for $T < T_\lambda$. This asymmetry is a violation of scaling if these exponents correctly describe $C_{p\phi}$ arbitrarily close to the λ line. The small residual x dependence of these exponents, if real, would be in violation of universality. To explore how serious these violations are one could attempt an analysis in which higher-order terms would be allowed to contribute to Eq. (12). We have not attempted such analysis at this time. We note, however, that in the analogous case of the λ line in P-T space at $x = 0$, a simple-power-law assumption for C_p also yielded[38] the result that the branch for $T > T_\lambda$ tended to have a more positive exponent than the branch for $T < T_\lambda$. This discrepancy, which is especially clear at higher pressures, can be removed[39] by the addition of higher-order terms to the functional form which describes the specific heat. Nevertheless, one retains the disagreement with scaling in the sense that the amplitude of the specific heat is pressure dependent. It would seem then that, both for the λ line in the p-T plane (with $x = 0$) and the λ line in the x-T plane ($p \cong 0$), small but persistent deviations from scaling occur.

We finally note that, in spite of these deviations, our result of a negative α' is consistent with the scaling relationship[47] $\zeta = \frac{1}{3}(2 - \alpha')$, where ζ is the exponent which characterizes the vanishing of the superfluid density at T_λ. Using the value of $\zeta = 0.672$ which has been recently reported by Ahlers[48] as being independent of concentration at least for a region not too close to the tricritical point, one obtains $\alpha' = -0.016$. All our values of α' are within one standard deviation of this value.

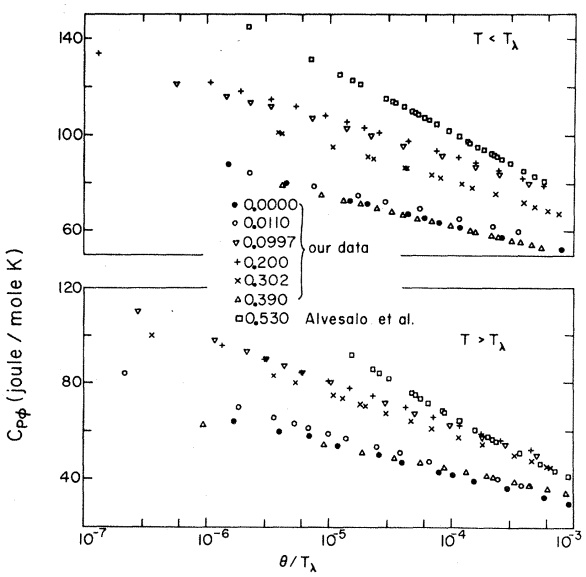

FIG. 17. $C_{p\phi}$ as a function of θ for $T < T_\lambda$ and $T > T_\lambda$.

VI. OTHER THERMODYNAMIC DERIVATIVES

Having obtained the behavior of $C_{p\phi}$ as a function of θ, it is relatively easy to obtain the behavior of $(\partial x/\partial T)|_{p,\phi}$ and $(\partial x/\partial\phi)|_{p,T}$, the other derivatives which behave as $C_{p\phi}$ near T_λ. The values we compute for these derivatives will be subject to direct checks from osmotic pressure measurements which are now in progress.[49] $(\partial x/\partial T)|_{p,\phi}$ is given by Eq. (7), and hence all one has to do is use Eq. (12) with the accompanying parameters $C_{p\phi}$ given in Table III. Equivalently, we have used Eq. (18) to obtain a plot of x-x_λ along paths of constant ϕ. This is shown in Figs. 18 and 19. The lines in this graph extend only within the range of data used in determining $C_{p\phi}$. The slight curvature visible on some of these lines reflects the θ dependence in the curly bracket of Eq. (19).

To obtain $(\partial x/\partial\phi)|_{p,T}$ we used the equation

$$\left.\frac{\partial x}{\partial\phi}\right|_{p,T} = \left.\frac{\partial x}{\partial\phi}\right|_{p,\phi} - \left.\frac{\partial x}{\partial T}\right|_{p,\lambda}\left.\frac{\partial T}{\partial\phi}\right|_{p,\lambda}, \tag{21}$$

where we again take the λ derivatives with their values at the λ line. This equation gives $(\partial x/\partial\phi)|_{p,T}$ on a path of $\phi = \text{const}$ if one uses on the right-hand side Eq. (7) for $(\partial x/\partial T)|_{p,\phi}$. If one wants $(\partial x/\partial\phi)|_{p,T}$ as a function of $x - x_\lambda$ for its "natural" path of $T = \text{const}$ we further have to compute

$$(x - x_\lambda)_T = (x - x_\lambda)_\phi + \theta T_\lambda \left.\frac{\partial x}{\partial T}\right|_{p,\lambda}, \tag{22}$$

which can easily be derived from a diagram similar to Fig. 15. In Eq. (22) the subscript on $x - x_\lambda$

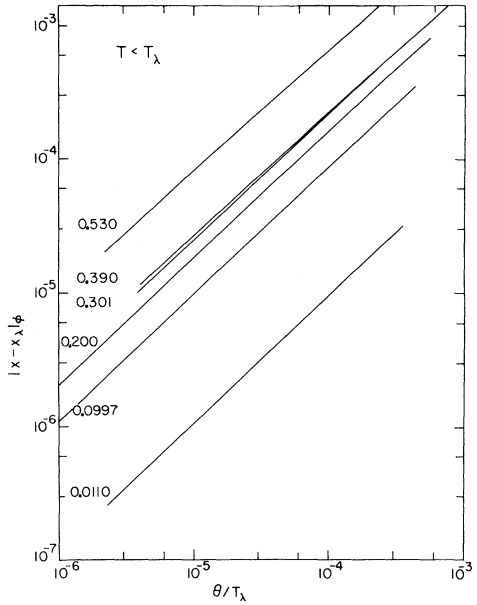

FIG. 18. Paths of constant ϕ for $T<T_\lambda$. These are calculated from $C_{p\phi}$ and the λ parameters.

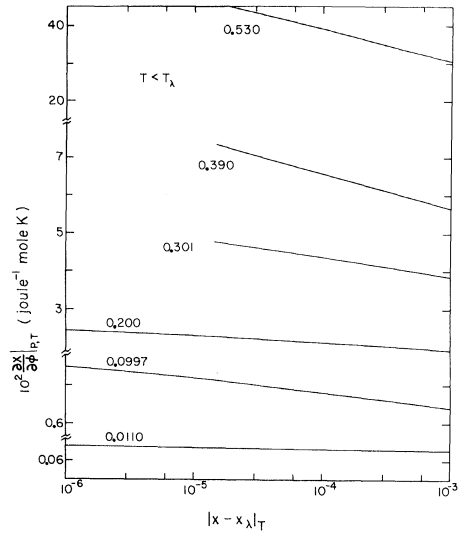

FIG. 20. Derivative $(\partial\phi/\partial x)|_{p,T}$ for $T<T_\lambda$ as calculated from $C_{p\phi}$ and the λ parameters at various mole fractions, x_λ. The smallest scale division on the abscissa is 0.1 J/mole K at $x=0.530$; 0.01 J/mole K at $x=0.390$, 0.301, and 0.200; 0.001 J/mole K at $x=0.0997$; and 10^{-4} J/mole K at $x=0.0110$.

indicates the path along which this quantity is measured. In calculating $(\partial x/\partial\phi)|_{p,T}$ the x dependence of $(\partial x/\partial T)|_{p,\phi}$ and the λ parameters was not considered. This is in the same spirit as the calculation for $C_{p\phi}$, where it was found to be negligible. The result for $(\partial x/\partial\phi)|_{p,T}$ is shown in Figs. 20 and 21 plotted versus $(x-x_\lambda)_T$. The T in this path can be taken to be the λ temperature to the same approximation that $C_{p\phi}$ along different values of ϕ was verified to be $C_{p\phi}$ along ϕ_λ.

VII. SUMMARY

We have presented in this paper our measurements of the specific heat of ^{4}He and ^{3}He-^{4}He mix-

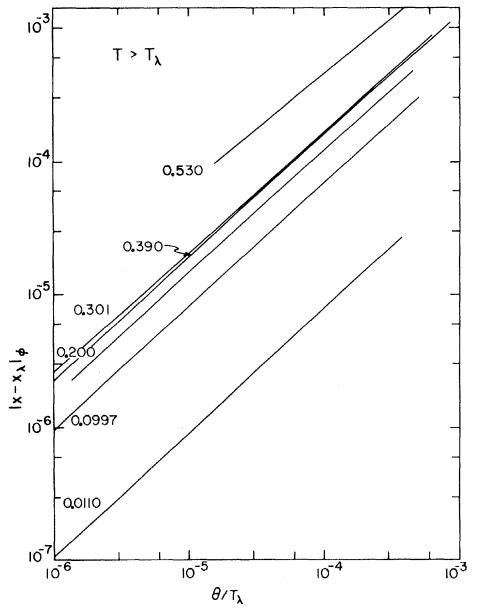

FIG. 19. Paths of constant ϕ for $T>T_\lambda$. These are calculated from $C_{p\phi}$ and the λ parameters.

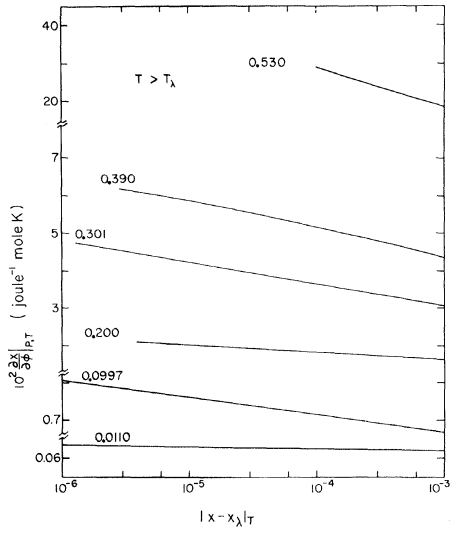

FIG. 21. Derivative $(\partial\phi/\partial x)|_{p,T}$ for $T>T_\lambda$ as calculated from $C_{p\phi}$ and the λ parameters at various mole fractions, x_λ. The smallest scale division on the abscissa is 0.1 J/mole K at $x=0.530$; 0.01 J/mole K at $x=0.390$, 0.301, and 0.200; 0.001 J/mole K at $x=0.0997$; and 10^{-4} J/mole K at $x=0.0110$.

tures at their λ transition for ^{3}He mole fractions less than about 0.4. We have discussed our experimental apparatus and procedure as well as our investigation of the difference between our measurements along a path of liquid-vapor coexistence and the specific heat at constant pressure and mole fraction. We found that for the range of data analyzed in this paper this difference is negligible.

Our data analysis for ^{4}He confirms some of the work of Ahlers, although it differs somewhat in detail. We find that the branches of the specific heat above and below T_λ, when fitted to a simple power law, show an asymmetry with characteristic exponents of $+0.012$ and -0.012, respectively. We find that this asymmetry persists with the mixtures in the sense that one branch tends to be more singular than the other. For the mixtures, the data show the effect of path renormalization which causes the heat capacity to reach a finite value at the transition. A simple-power-law analysis of the data does not yield the true renormalized exponents, but rather effective exponents which for the same range of data from T_λ tend to become more and more negative. In order to verify the conjectured universal behavior of the conjugate specific heat $C_{p\phi}$, we have constructed this specific heat using our data and our calculation of the thermodynamic derivatives at the λ line: $(\partial x/\partial T)|_{p,\lambda}$, $(\partial\phi/\partial T)|_{p,\lambda}$, $(\partial s/\partial T)|_{p,\lambda}$. We have extended this analysis to the data at $x=0.53$ of Ref. 6. We find that $C_{p\phi}$, when tested with a simple power law, does indeed show a universal character in its exponents, although in details it retains the asymmetry observed in ^{4}He, which is in violation of scaling.

We have also calculated the paths of constant ϕ on the x-T plane and the derivative $(\partial x/\partial\phi)|_{p,T}$, which are closely related to $C_{p\phi}$.

Our main qualitative results are shown in Figs. 1, 8, 9, and 17 for the renormalized and unrenormalized specific heats. The main quantitative results are given in Tables II and III for the power-law parameters of the two specific heats.

ACKNOWLEDGMENTS

We would like to thank Professor W. Zimmermann, Jr. of the University of Minnesota for many helpful discussions on our work, and for making the specific-heat data at $x=0.53$ available to us. We also would like to thank P. Steinback for his help in the early part of the data analysis and M. DiPirro for his help in the later stages.

APPENDIX

We derive in the Appendix an equation for obtaining the liquid specific heat C_{px} from measurements in a container of fixed volume with a two-component liquid and vapor in equilibrium. If we ignore surfaces and interfaces the total entropy S is given by

$$S=n_l s_l+n_v s_v\ . \tag{A1}$$

Differentiating this expression with respect to T we obtain

$$\frac{dS}{dT}\equiv\frac{C_m}{T}=n_l\frac{ds_l}{dT}+(s_l-s_v)\frac{dn_l}{dT}+(n-n_l)\frac{ds_v}{dT}\ , \tag{A2}$$

where the total derivatives are along the experimental path in which the molar concentration and the pressure are changing in a way unique to the amount of liquid and vapor present. If we consider $s_l=s_l(x_l,p,T)$ we can write

$$\frac{ds_l}{dT}=\left.\frac{\partial s_l}{\partial T}\right|_{p,x_l}+\left.\frac{\partial s_l}{\partial p}\right|_{T,x_l}\frac{dp}{dT}+\left.\frac{\partial s_l}{\partial x_l}\right|_{p,T}\frac{dx_l}{dT}\ . \tag{A3}$$

We can change two of the partial derivatives in Eq. (A3) by using the Maxwell relations

$$\left.\frac{\partial s}{\partial p}\right|_{T,x}=-\left.\frac{\partial v}{\partial T}\right|_{p,x},\qquad \left.\frac{\partial s}{\partial x}\right|_{p,T}=-\left.\frac{\partial\phi}{\partial T}\right|_{p,x}, \tag{A4}$$

which are obtained from the differential of the molar Gibbs free energy $dg=-s\,dT+v\,dp+\phi\,dx$, with $\phi=\mu_3-\mu_4$ the difference in the molar chemical potentials of ^{3}He and ^{4}He. Using Eqs. (A4) in Eq. (A3) we obtain

$$\frac{ds_l}{dT}=\frac{C_{px}}{T}-\left.\frac{\partial v_l}{\partial T}\right|_{p,x_l}\frac{dp}{dT}-\left.\frac{\partial\phi}{\partial T}\right|_{p,x_l}\frac{dx_l}{dT}\ , \tag{A5}$$

where for simplicity we omit the subscript l on C_{px}. If we consider $x_l=x_l(T,p,\phi)$, then we can write the total derivative in Eq. (A5) as

$$\frac{dx_l}{dT}=\left.\frac{\partial x_l}{\partial T}\right|_{p,\phi}+\left.\frac{\partial x_l}{\partial p}\right|_{T,\phi}\frac{dp}{dT}+\left.\frac{\partial x_l}{\partial\phi}\right|_{p,T}\frac{d\phi}{dT}\ . \tag{A6}$$

Also from the Gibbs-Duhem relationships for vapor and liquid,

$$\begin{aligned}0&=-s_l\,dT+v_l\,dp-x_l\,d\phi-d\mu^4\ ,\\ 0&=-s_v\,dT+v_v\,dp-x_v\,d\phi-d\mu^4\ ,\end{aligned} \tag{A7}$$

we obtain upon subtraction

$$\frac{d\phi}{dT}=\left(\Delta v\frac{dp}{dT}-\Delta s\right)\frac{1}{\Delta x}\ , \tag{A8}$$

where $\Delta v=v_l-v_v$, etc. We now use Eqs. (A8), (A6), and (A5) in (A2) and obtain

$$\begin{aligned}\frac{(1/n_l)C_m-C_{px}}{T}&=-\left.\frac{\partial v_l}{\partial T}\right|_{p,x_l}\frac{dp}{dT}-\left.\frac{\partial\phi}{\partial T}\right|_{p,x_l}\\ &\times\left[\left.\frac{\partial x_l}{\partial T}\right|_{p,\phi}+\left.\frac{\partial x_l}{\partial p}\right|_{T,\phi}\frac{dp}{dT}+\left.\frac{\partial x_l}{\partial\phi}\right|_{p,T}\left(\Delta v\frac{dp}{dT}-\Delta s\right)\frac{1}{\Delta x}\right]\\ &+\frac{\Delta s}{n_l}\frac{dn_l}{dT}+\frac{n-n_l}{n_l}\frac{ds_v}{dT}\ .\end{aligned} \tag{A9}$$

We then use the following identities:

$$\left.\frac{\partial\phi}{\partial T}\right|_{p,x}=-\left.\frac{\partial x}{\partial T}\right|_{p,\phi}\left.\frac{\partial\phi}{\partial x}\right|_{p,T}\ ,$$

$$\left.\frac{\partial x}{\partial p}\right|_{T,\phi} = -\left.\frac{\partial \phi}{\partial p}\right|_{T,x} \left.\frac{\partial x}{\partial \phi}\right|_{p,T}, \tag{A10}$$

and obtain

$$\frac{(1/n_l)C_m - C_{px}}{T} = -\left.\frac{\partial v_l}{\partial T}\right|_{p,x_l} \frac{dp}{dT} - \frac{\Delta s}{n_l}\frac{dn_l}{dT} + \frac{n-n_l}{n_l}\frac{ds_v}{dT} - \left[\left.\frac{\partial \phi}{\partial T}\right|_{p,x_l} + \left.\frac{\partial \phi}{\partial p}\right|_{x_l,T}\frac{dp}{dT} - \left(\Delta v \frac{dp}{dT} - \Delta s\right)\frac{1}{\Delta x}\right]\left.\frac{\partial x_l}{\partial T}\right|_{p,\phi}. \tag{A11}$$

This is a suitable working equation giving us the difference between the measured specific heat C_m/n_l and C_{px}, which is the quantity of interest. In this equation we have isolated the derivative $(\partial x_l/\partial T)|_{p,\phi}$ which is possibly singular. This can be seen from Eq. (7) in Sec. II, in which this derivative is related to $C_{p\phi}$.

To evaluate the right-hand side of Eq. (A11) we used the vapor-pressure data of Sydoriak and Roberts,[12] the molar-volume data of Kerr,[48] and the estimate of the excess chemical potentials of Roberts and Swartz.[15] The vapor properties were computed using an ideal-gas approximation. For the liquid mixture's entropy we integrated heat-capacity data, up to the λ temperature.[2,13] For $(\partial x_l/\partial T)|_{p,\phi}$ we used Eq. (7) along with values of $C^x_{p\phi}$ obtained via Eq. (3).

A simpler equation than Eq. (A11) was also used in estimating the difference between C_m and C_{px}:

$$\frac{(1/n_l)C_m - C_{px}}{T} = -\left.\frac{\partial v_l}{\partial T}\right|_{p,x_l}\frac{dp}{dT} + \frac{n-n_l}{n_l}\frac{ds_v}{dT} + \left[-\left.\frac{\partial \phi}{\partial T}\right|_{p,x_l}\left(\frac{1-x_l}{n_l}\right) + \frac{\Delta S}{n_l}\right]\frac{dn_v}{dT}. \tag{A12}$$

This equation is useful away from T_λ, where one does not have to worry about possible singularities. It can easily be derived by using the expression

$$\frac{dx_l}{dT} \simeq -\frac{1-x_l}{n_l}\frac{dn_v}{dT}, \tag{A13}$$

which assumes most of the atoms evaporating from the liquid are ^{3}He.

---

*Research supported in part by the National Science Foundation under Grant No. GP 7146.

†Work represents in part research performed by this author in partial fulfillment of the PhD requirements at the University of Minnesota.

‡Present address: Heat Division, National Bureau of Standards, Washington, D.C. 20234.

[1]W. M. Fairbank, M. J. Buckingham, and C. F. Kellers, in *Proceedings of the Fifth International Conference on Low Temperature Physics, Madison, Wisc.*, 1957, edited by J. R. Dillinger (Univ. of Wisconsin, Madison, Wisc., 1958), p. 50. M. J. Buckingham and W. M. Fairbank, in *Progress in Low Temperature Physics*, edited by C. J. Gorter (North-Holland, Amsterdam, 1961), Vol. III, p. 83; C. F. Kellers, thesis (Duke University, 1960) (unpublished).

[2]R. de Bruyn Ouboter, K. W. Taconis, C. le Pair, and J. J. M. Beenakker, Physica 26, 853 (1960).

[3]K. W. Taconis and R. de Bruyn Ouboter, in *Progress in Low Temperature Physics*, edited by C. J. Gorter (North-Holland, Amsterdam, 1964), Vol. IV, p. 38ff.

[4]V. N. Grigor'ev, B. N. Esel'son, E. A. Masimov, G. A. Mikhailov, and P. O. Novikov, Zh. Eksp. Teor. Fiz. 55, 1160 (1968) [Sov. Phys.–JETP 28, 605 (1969)].

[5]F. M. Gasparini and M. R. Moldover, Phys. Rev. Lett. 23, 749 (1969).

[6]T. A. Alvesalo, P. M. Berglund, S. T. Islander, G. R. Pickett, and W. Zimmermann, Jr., Phys. Rev. A 4, 2354 (1971).

[7]M. E. Fisher, Phys. Rev. 176, 257 (1968). For similar considerations on the effect of critical exponents as a function of thermodynamics path see B. J. Lipa and M. J. Buckingham, Phys. Lett. A 26, 643 (1968).

[8]M. E. Fisher and P. E. Scesney, Phys. Rev. A 2, 285 (1970).

[9]B. J. Lipa and M. J. Buckingham, in Ref. 7.

[10]R. B. Griffiths and J. C. Wheeler, Phys. Rev. A 2, 1047 (1970).

[11]G. Ahlers, Phys. Rev. Lett. 23, 464 (1969); Phys. Rev. A 3, 696 (1971).

[12]M. J. Buckingham and W. M. Fairbank, in Ref. 1; see also A. B. Pippard, *The Elements of Classical Thermodynamics* (Cambridge U.P., New York, 1966), p. 136ff.

[13]S. G. Sydoriak and T. R. Roberts, Phys. Rev. 118, 901 (1960).

[14]D. O. Edwards, D. F. Brewer, P. Seligman, M. Skertic, and M. Yaqub, Phys. Rev. Lett. 15, 773 (1965).

[15]E. A. Guggenheim, *Thermodynamics*, (North-Holland, Amsterdam, 1967), p. 187ff.

[16]T. R. Roberts and B. V. Swartz, in *Proceedings of the Second Symposium on Liquid and Solid He*^{3} (Ohio State U.P., Columbus, Ohio, 1960). There are many references given here to other computations of excess thermodynamic quantities as well as to comparisons of experimental data with theories of mixtures.

[17]J. C. Wheeler and R. B. Griffiths, Phys. Rev. 170, 249 (1968).

[18]A similar arrangement has also been used by W. R. Gardner, J. K. Hoffer, and N. E. Phillips [Phys. Rev. A 7, 1029 (1973)].

[19]This calorimeter bottom is the same as that used by M. Moldover for measurements at the critical point of ^{3}He and ^{4}He; see M. R. Moldover, Phys. Rev. 182, 342 (1969).

[20]Servometer Corp., 82 Industrial East, Clifton, N.J. 07012.

[21]W. B. Driver Co., P.O. Box 1467, Orangeburg, S. C. 39115.

[22]CryoCal Inc., 1317 Ave. E, Riviera Beach, Fla. 33404.

[23]James G. Biddle Co., Township Line and Jolly Road, Plymouth Meeting, Pa. 19462.

[24]Monsanto Research Corp., Mound Laboratory, Miamis-

burg, Ohio.
[25]Power Supply 610A from Hewlett Packard Corp., 39 Saginaw Drive, Rochester, N. Y. 14623.
[26]Differential voltmeter Model 881 AB from John Fluke Mfg. Co. Inc., P. O. Box 7428, Seattle, Wash. 98113.
[27]Frequency counter Model 101A from Monsanto Research Corp.
[28]This bridge is similar to the one used by Kierstead; see H. A. Kierstead, Phys. Rev. 153, 258 (1967).
[29]Transformer No. 8314 from James Electronics Inc., 4050 North Rockwell St., Chicago, Ill. 60618.
[30]Transformer model ST-100A from Singer Instrumentation, 3211 South La Cienega Blvd., Los Angeles, Calif. 90016.
[31]Ratio-transformer model 1011 from Singer Instrumentation.
[32]Model HR-8 lock-in detector from P. A. R. Corp., P. O. Box 2565, Princeton, N. J. 08540.
[33]Model G-1010 chart recorder from Varian Assoc., 611 Hansen Way, Palo Alto, Calif. 94303.
[34]F. G. Brickwedde, H. van Dijk, M. Durieux, J. R. Clement, and J. R. Logan, 1958 *He^4 Scale of Temperatures*, Natl. Bur. Std. Publ. (U. S. GPO, Washington, D. C., 1960).
[35]T. R. Roberts, R. H. Sherman, S. G. Sydoriak, and F. G. Brickwedde, in Ref. 3, p. 480.
[36]E. C. Kerr and R. D. Taylor, Ann. Phys. (N. Y.) 26, 292 (1964).
[37]For details of this calculation see F. M. Gasparini, PhD thesis (University of Minnesota, 1970) (unpublished); available in microfilm.
[38]R. W. Hill and O. V. Lounasmaa, Phil. Mag. 2, 142 (1957).
[39]G. Ahlers, Phys. Rev. A 1, 530 (1973).
[40]B. Widom, J. Chem. Phys. 43, 3898 (1965).
[41]L. P. Kadanoff, Physics 2, 263 (1966).
[42]P. R. Bevington, *Data Reduction and Error Analysis for the Physical Sciences* (McGraw-Hill, New York, 1969), p. 189.
[43]The results of this calculation have also been reported by F. M. Gasparini and M. R. Moldover, in *Low Temperature Physics-LT* 13, edited by K. D. Timmerhaus, W. I. O'Sullivan, and E. F. Hammel (Plenum, New York, 1974), Vol. 1.
[44]P. C. Hohenberg and M. Barmatz, Phys. Rev. A 6, 289 (1972); S. C. Greer, T. E. Block, and C. M. Knobler (unpublished).
[45]The universal behavior of α and α' for $C_{p\phi}$ has been explicitly assumed by Fisher (Ref. 7) and has been more recently discussed in more general terms by R. Griffiths [Phys. Rev. Lett. 24, 1479 (1970)] and L. P. Kadanoff, in *Proceedings of the International School of Physics "Enrico Fermi", Course LI*, edited by M. S. Green (Academic, New York, 1973).
[46]The ratio of t/θ has also been calculated for $T<T_\lambda$ by G. Ahlers, Phys. Rev. A 10, 1670 (1974). His calculation is performed in $\phi - T$ space rather than $x - T$ space. We are in good agreement with this calculation.
[47]B. D. Josephson, Phys. Lett. 21, 608 (1966).
[48]G. Ahlers, Phys. Rev. A 10, 1670 (1974).
[49]C. A. Gearhart, Jr. and W. Zimmermann, Jr., Phys. Lett. A 48, 49 (1974), and unpublished.